Late Pleistocene New Jersey Shelf Sedimentation as a Response to Glacio-eustatic Sea Level Rise

by

Stanley B. Stackhouse, B.S.;B.S.

Thesis

Presented to the Faculty of the Graduate School

Of the University of Texas at Austin

in Partial Fulfillment

of the Requirements

for the Degree of

Master of Science in Geological Sciences

The University of Texas at Austin

August 2009

The Thesis committee for Stanley B. Stackhouse certifies that this is the approved version of the following thesis:

Late Pleistocene New Jersey Shelf Sedimentation as a Response to Glacio-eustatic Sea Level Rise

Approved By

Supervising Committee:

Supervisor: _____

William L. Fisher

_____

John A. Goff

_____

Ronald J. Steel

Dedicated to Cammy, daddy’s little girl

ACKNOWLEDGEMENTS

Completing a thesis takes strong dedication as well as an even stronger support group. I first would like to thank God for whom all credit all my achievements thus far. I would also like to thank my parents, grandparents, siblings, friends, and significant other for there continued support. Next, I would like to thank the University of Texas and all of its associated institutes for their monetary and educational support. I would like to offer thanks to my committee members for their guidance and input. Special thanks goes out to my co-advisor John Goff for making the 2007 KN190 cruise a success, as we were faced with much adversity during the expedition. Lastly, but most certainly not least, I would also like to give a special thanks to my other co-advisor William L. Fisher for all of his support and aid while I attended the University of Texas.

Stanley B. Stackhouse

Late Pleistocene New Jersey Shelf Sedimentation as a Response to Glacio-eustatic Sea Level Rise

by

Stanley B. Stackhouse, MSGeoSci

The University of Texas at Austin, 2009

CO-SUPERVISORS: William L. Fisher and John Goff

Shallowly-buried channel systems have been imaged on the New Jersey Shelf with high-resolution seismic imaging. These channels formed as riverine systems that occupied the exposed shelf during the Last Glacial Maximum, ~18 ka. Subsequent sea level rise ~15-12 ka modified the valleys, forming estuaries and filling the channels with estuarine sediments. The infill sediments within the channel provide evidence for the response of the shelf to the Late Pleistocene glacio-eustatic sea level rise, but little work has been done on samples from these strata. This study aids in the ground-truthing of previous stratigraphic results by analyzing the cores collected within the infill sediments. The seismic stratigraphy of fill sediments from the mid-shelf and outer-shelf channels are structurally dissimilar. The mid-shelf channel fill stratigraphy is dominated by finely-laminated U-shaped reflectors throughout the section, with cut and fill geometries. In contrast, the outer shelf channel fill stratigraphy is a well-ordered sequence of 4 identifiable, primarily flat-lying seismic units. We collected five cores in mid-shelf channels (~30 m water depth), one in an outer shelf channel (~80 m of water depth) and one core in the trangressive ravinement surface. Cores were logged for density and seismic velocity. Grain size analysis was conducted by settling column and laser particle size analyzer. Radiocarbon analysis of the stratigraphy was conducted with the shell fragments and organic mud within the samples. The foraminiferal assemblages

aided in determining the depositional environment. Using these data I investigated the differences in depositional environment of the mid- and outer-shelf channels systems, and consider these results in the context of sedimentary models for estuarine processes. The radiocarbon dates and foraminiferal are consistent with channel infill in an estuarine environment. Grain size and density log data indicate that the mid-shelf channel fills are sandier than the outer-shelf channel fills, which leads me to infer that the sediment from the mid-shelf channels was deposited in a higher energy environment than that of the sediment in the outer shelf channels. The stratigraphic differences and locations of the channel systems are similar to the Zaitlin (1994) model of incised valley infill, but infill of the mid-shelf channel system could possibly be the result of a catastrophic meltwater flood event occurring ~14 ka as glacial lakes to the north broke their dams and flooded the mid-shelf.

Table of Content

Figures

Tables

1.0 INTRODUCTION

The shallowly- buried river channel systems on the New Jersey continental shelf (Figure 1) comprise important evidence of the shelf's response to the most recent glacio-eustatic sea-level rise. Before this transgression, the continental shelf had been a subaerial coastal plain. The regional geology of the New Jersey shelf otherwise does not completely record this response because it has been modified by the subsequent trangressive ravinement. The strata within the channels are interpreted as estuarine sediments that back-filled the paleo-channels as transgression proceeded (Nordfjord et al., 2006). These strata have been imaged extensively with high-resolution Huntec boomer and chirp seismic data (Davies et al., 1992; Sheridan et al., 2000; Duncan et. al., 2000). However, there has been less work done on sediment samples (Buck et al., 1999; Duncan 2000; Christensen et al., 2007).

This study aids in the groundtruthing of previous seismic stratigraphic work done on the New Jersey shelf by analyzing cores collected in the summer of 2007. The targeted infilled channels are characterized as part of an ancient coastal plain that developed on the exposed shelf during the Last Glacial Maximum (LGM) ~18 ka (Davies et al., 1992). As sea level rose ~15-10 ka these channels were back-flooded and modified into estuaries. The Allen and Posamentier (1993) stratigraphic model suggests that transgressive estuarine deposits follow an ordered sequence: (1) fluvial lag deposits, (2) estuarine sands and muds, (3) basin fill mud, and (4) estuarine mouth complex sediments. For

the outer and mid- shelf area off New Jersey, there are two noticeably different stratigraphic geometries for these sediments (Figure 2a & 2b).

In the outer shelf channels (currently ~80 m waters depth) the seismic character of the infill shows different seismic facies bounded by horizontal boundaries (Figure 2a; Nordjford et al., 2006). Nordfjord and co-authors identified each of the different facies that were associated with the different depositional zones of the Allen and Posamentier (1993) model. In the mid-shelf channels (currently ~30 m water depth) the channel fill stratigraphy shows finely laminated, U-shaped layering throughout the section, with cut-and-fill deposits (Figure 2b).

The differences in the stratigraphic geometries of the mid- and outer shelf channels are a prime motivating factor for investigating, through core-based analysis, the infill sediment of these channels. What differences in depositional conditions could have resulted in such differing stratigraphic geometries? Are the mid- and outer-shelf channel fill sediments part of the same depositional system, or are they distinctly separate events resulting from different depositional environments? My hypothesis is that the mid-shelf channel fill sediment were deposited in a relatively higher energy environment than the outer shelf channel system and that the outer shelf channel system was infilled prior to the infilling of the mid-shelf channel. The U-shaped (Figure 2b) geometries of the mid-shelf channel fill show intervals that I infer to be indicative of down-cutting and filling (Duncan, 2001), which would suggest a higher energy system than that of the

outer shelf channel infill strata that are relatively flat-lying (Figure 2a). The cut-and-fill morphology that occurs along the mid-shelf channel flanks suggests autogenic lateral accretion within the channel (Galloway and Hobday, 1996; Blum and Tournqvist, 2000). Recent researchers (Fulthorpe and Austin, 2004; Donnelly et at. 2005; Theiler et al. 2007) have explored the possibility of erosion and deposition across the New Jersey shelf as a function of a catastrophic meltwater flood events ~5,000 to ~10,000 yr after the LGM as glacial lakes to the north of the study area broke through their glacial dams. This theory is important to my study because it could possibly explain the nature of the deposition of the mid-shelf channel infill sediments.

In this study, I will ground-truth previous seismic stratigraphic work done by Nordfjord et al. (2006) (Figure 2a). I will achieve this by analyzing the grain size of the cored sediment that penetrated the outer shelf channel and determining whether or not the sediment is similar to the lithologic descriptions from Nordfjord et al. (2006). I will also analyze the grain size from the cores within the mid-shelf channel (Figure 2b) to determine the nature of the sediment there. I will also place the sediment from both locations within a sequence stratigraphic framework using radiocarbon age dating and the observed seismic stratigraphy. I will explore two depositional models for the mid-shelf channels: (1) back (landward)-stepping sedimentation as estuarine conditions took over the shelf, and (2) deposition as a function of a catastrophic post-LGM meltwater flood event(s).

2.0 Background

2.1 Study Area

The Barnegat Corridor is a dip transect crossing the New Jersey shelf, in the Mid-Atlantic Bight, extending seaward from the Barnegat Inlet (Duncan et al., 2000; [Figure 1]). The shelf at this location is ~150 km-wide and slopes seaward at ~0.06° (Swift et al. 1980; Davies et al. 1992). The terminal moraines of the Laurentide Ice Sheet associated with the late Wisconsin glaciation have been mapped ~120 km to the north of this study area in northern Long Island (Schlee and Pratt, 1970; Stone and Borns, 1986). The shelf can be divided into inner, mid-, and outer shelf components (Goff et at., 1999; Duncan, 2001): the inner shelf is landward of the 20 m isobath; the middle shelf is from ~20-50 m water depth, with the seaward edge defined by a mid-shelf scarp (Figure 3a); and the outer shelf is seaward of the 50 m isobath to the shelf edge (Figure 3b).

The regional stratigraphy of the New Jersey shelf provides evidence for spatial and temporal variations in the sediment supply, deposition processes, and accommodation (Gulick et al. 2005). There is a regional reflector “R” that has been identified by Duncan et al. (2000) as the regressive ravinement surface and which is eroded by presumed fluvial channels. Further out on the shelf the “R” reflector forms the base of the outer shelf wedge (Milliman et al. 1990). There is also another late Pleistocene-Holocene mid-shelf wedge (Ewing et al., 1963; Knott and Hoskins, 1968; Knebel and Spiker, 1977; Harris, 1983; Milliman et al.,

1990). These deposits help establish the position of the successive channel fill in the mid- and outer shelf channel systems that are the object of this study.

2.2 Incised Valleys and Initial Formation of Estuaries

The relationship between incised valley formation and the sediment infill of those valleys is important when trying to place sediment within a sequence stratigraphic framework in an area that has been interpreted as an estuarine environment. The cutting of incised valleys is associated with fluvial erosion during relative sea-level fall, either caused by a eustatic change or some other local factor creating such fall (i.e., tectonics) (Dalrymple et al., 1994). The sediment fill within the valley may be partly a product of deposition associated with the relative sea-level fall. Most of the filling, however, is likely a product of the relative sea-level rise or transgressive systems tract that follows valley incision, as the shoreline moves back landward and estuarine conditions are created. Valley filling takes place in three ways and is dependent upon the controls on deposition (Schumm, 1977; Schumm et al. 1994): (1) Progressive backfilling during relative sea-level rise, (2) progressive down-cutting and filling of the valley due to uplift and/or changes in climate that increase the sediment supply significantly, and (3) vertical filling caused by an increase in sediment supply, again most like caused by a climate change.

Estuaries were originally defined based on their salinities (Pritchard 1967), but I will define them based on Dalrymple et al. (1992) as the seaward end of a

drowned valley system that receives sediment input from marine and fluvial sources with facies that are influenced by tidal, wave, and fluvial processes (Figure 4). In an estuarine system, the sediment infill is developed gradually by the backfilling of sediment during a relative sea-level rise. However, estuaries receive clastic sediments from two sources: marine and terrestrial. Only when the sea-level rise is more than the output of sediment does shoreline transgression and back filling begin (Curray, 1964; Boyd et al., 1992).

Zaitlin et al. (1994) have developed a three-fold subdivision that represents the depositional organization of an infilling incised valley as it evolves through time during transgression: segments I, II, and III (Figure 4). Segment I is the outer incised valley. This segment, during falling sea level, is a bypass area but, as sea level rises, estuarine conditions are established. Generally, there is a systematic deposition of a basal fluvial lag deposit that is overlain by very muddy central basin deposits as transgression proceeds. Overlying the central basin mud deposits are the sandier estuarine mouth complex sediments. Estuarine mouth complex sediments could be a lateral variation of sedimentary facies such as tidal inlets to washovers, flood-tidal deltas, and/or barrier beach sands (Dalrymple et al., 1992; Zaitlin et al., 1994; Masselink and Hughes 2003; Nordfjord et al., 2006). The contact between the two facies is usually marked as an irregular and discontinuous tidal ravinement surface (Allen and Posamentier 1993). The estuarine sediments in this segment are eroded by the wave ravinement surface that forms due to wave erosion as sea level continues to rise.

Segment II is the middle incised valley located between the seaward end of segment I and the estuarine maximum flooding limit (Figure 4). This segment is similar to segment I, because it is a bypass area that evolves as sea level rises. Fluvial lag deposits overlie the erosive base of the channel and are overlain by transgressive/estuarine facies, which vary along the segment (Dalyrmple et al., 1992). This variance between the sediments establishes a difference between the segments I and II proposed by Zaitlin et al. (1994). Segment III is located between the estuarine limit and the landward limit of incision. The infill is typically entirely fluvial and has developed through various channel morphologies. The sedimentation rate is a function of sea-level rise and accommodation (Figure 4).

2.3 Catastrophic Meltwater Event History and Timing

According to Thieler et al. (2007), as the Laurentide Ice Sheet began to retreat from its maximum position, glacial lakes in what is now New Jersey and New York, lakes Bayonne and Hackensack, began draining water through spillways in the terminal moraine (Figure 5). As the ice retreat continued to the north, Hell Gate in the East River east of Manhattan deglaciated, and initiated the drainage of the Hudson River basin into Lake Connecticut (Stanford and Harper, 1991). The draining of Lakes Hudson, Albany, and Vermont, which all are a part of the Hudson River basin, as well as Lake Iroquois through the Mohawk Valley came through the Hell Gate's route (Muller and Prest, 1985; Pair and Rodrigues,

1993). The majority of the meltwaters likely drained southward through the Mohawk Valley to breach the Narrows, while some of the meltwaters likely flowed eastward through Connecticut. Ridge (1997) has stated that this drainage pathway continued until after 12,000 year BP. Reconstruction of the drainage routing history by Stanford and Harper (1991) suggests that no meltwater exited the Hudson River to the south across the New York–New Jersey shelf until the breach at the Narrows (Figure 5).

Fulthorpe and Austin (2004) have identified and mapped some buried incisions which they presumed to be fluvial in origin, in an area south-southeast of the mid-shelf channel system in my study area (Figure 1). They suspect that one or more of the catastrophic flood events outlined above created those channels. Thieler et al. (2007) have placed the timing of this catastrophic meltwater event between ~13,350 and ~12,000 years BP. As water from deglaciation broke through the Narrows creating dense gravity flows, the majority of the flood waters likely progressed down the Hudson Shelf Valley (HSV) and out onto the shelf possibly overflowing the banks of the HSV to flood the exposed shelf, as proposed by Fulthorpe and Austin (2004). Other flood waters were possibly redirected either to the north or south of the HSV (Figure 5).

Evidence for breach of the Narrows can be seen in some geological deposits and features. The sediment record in the lower HSV provides evidence for glacial outwash at the Narrows as the basal sediment has an age of ~12,000-12,500 yrs BP (Donnelly et al., 2005). Uchupi et al. (2001) found that the

morphology of the continental shelf off New York and New Jersey contains large sediment lobes that are oriented subparallel to the Hudson Shelf Valley. They suggest that the sediments were likely deposited when the meltwaters breached the Narrows dam and poured across the exposed shelf.

3.0 Methodology

In the summer of 2007, I was a part of a two-week coring expedition on the New Jersey shelf aboard the Woods Hole Oceanographic Institution's *R/V* Knorr. A mid-shelf channel system (Figure 2b) and an outer shelf channel system (Figure 1b) were targets of this research, along with the trangressive ravinement surface, the "T" seismic horizon (Figure 6). Each core was collected using a 20 ft/6 m vibracore configuration (Figure 7). As the cores were brought onboard, they were labeled, cut into 1.5 m sections, and each section was logged using the Multi-Sensor Core Logger (MSCL) for acoustic velocity (230 kHz), gamma-ray density and magnetic susceptibility. Some sections of core were split onboard and some visual lithological descriptions were performed to provide insight into the lithostratigraphy. Splitting of the cores onboard also functioned as an educational tool, as there were several undergraduate students working in the science party. Each core was placed into cold storage for the remainder of the cruise. Upon returning to port, core sections were transported to Lamont-Doherty Earth Observatory. Once there, all remaining sections were split and geologic descriptions were made. I then sampled the cores at various intervals of ~10 cm in homogenous intervals, with additional samples taken at lithological boundaries. Sample size was ~ 40 cc. During the sampling, any shell material and/or muds were separated for ^{14}C radiometric dating were separated and individually bagged. Each section of core was also digitally photographed twice, once using plain light and once using polarized light by the curatorial staff

of the LDEO Deep Sea Sample Repository. Polarized light photos revealed more details within the cores because the polarized light transmits more reflections than plain light. The cores were later scanned using X-ray radiography to help further identify any sedimentary structures not identified visually in the cores.

In order to analyze the core samples for grain size, each sample had to be prepared for analysis. A 250 ml labeled beaker was used to combine 2.55 g of sodium metaphospate and ~20 ml of deionized water. After which ~20-30 g of wet sediment was added to the solution and the solution was stirred continuously. The sample was then placed into a sonicator, which uses ultrasound energy to break up particles, for ~10-15 min, covered and allowed to set overnight in a beaker. The sample was then poured through a 62.4 μm sieve and a large funnel into a 1000 ml graduated cylinder. The sample was then rinsed with deionized water through the sieve and again collected in a 1000 ml graduated cylinder. The goal was to wash the clay and silt through the sieve and collect the slurry in the cylinder, without exceeding 1000 ml. In that case, the excess water was evaporated or siphoned off. Once the sediment in the sieve was clean, the sand was collected and placed in a pre-weighed aluminum pan and used in the settling tube analysis. The fine fraction slurry was bottled for analysis in the laser particle analyzer.

3.1 Grain Size Analysis via Settling Tube

The coarse fraction was analyzed for grain size in a settling tube. The sediment was placed on a closed gate at the top of a cylindrical tube that is 198cm in length and filled with water. The gate is connected to a computer system called the Femto J9211 Particle Sizing System (PSS). When the gate is opened, the sediment falls through into the column and the software begins to analyze the size of the particles as they begin to settle to the bottom. The particles have differential settling times as defined by Stoke's law (Folk, 1974), due to their variations in diameter. The grain distributions (in phi units, where grain size in mm = 2^{-phi}) of the various particles settling in the tube were measured by the computer software program. The total weight of the sediment was also measured by a scale that was connected to the base of the settling tube, as the sediment fell to the base of the column.

3.2 Laser Scattering Particle Size Distribution

The laser scattering particle size distribution analyzer called the Horiba LA-300, which has an internal laser source, was used to measure particle size distributions of the fine-grained fraction (<62.4μm). The instrument has a measurement range of 0.1-600 μm. Water was placed into the small chamber of the analyzer and was then circulated at ~500 ml/min. A small amount of the fine fraction slurry, ~1 ml, was pipetted out and placed in the small chamber with a

300 ml flow cell. Small increments of the slurry were added until the combination within the chamber was dense enough for the laser to analyze, as notified by the associated software. Once the slurry within the chamber was at an effective density, the slurry was then measured by the laser and particle size distributions displayed.

The laser analyzer works using laser diffraction technology. If the particle is larger than the wavelength of light, the light scatters from the edge of the particle at an angle that is a function of the size of the particle. The larger particles scatter light at smaller angles relative to light scattered from smaller particles. Observing the intensity of light scattered at different angles can determine the relative amounts of different size particles.

3.3 Age Determination

In order to place the cored sediments into a sequence stratigraphic framework properly, the absolute age of the sediments must be determined, if possible. I have approached finding the age of the sediment in various ways. I have used stable organic carbon primarily, which when calibrated correctly for its carbon source, is a useful tool for age dating. However, the calibration is complicated by the fact that the carbon present in the system can be marine, terrestrial, or recycled. In order to determine the nature of the source, δ13 values, which is the ratio of $^{13}C/^{12}C$, must be examined and determined. Marine

carbon typically has δ13 values of -21 +/- 1 $^{o}/_{oo}$ terrestrial carbon values are typically -27 +/- 1 $^{o}/_{oo}$ (Fry and Sherr, 1984).

Suitable shell fragments as well as mud from within the cored sediments were also sampled and sent to Arizona State University for radiocarbon (^{14}C) age dating. The ages of the shells, if they are not reworked or modern, constrain the age of sediment deposition. There were two shells that were age dated in this study (Table 1 and 2). Because the source of the carbon in the muds is unknown, the resulting radiocarbon dates were calibrated for both terrestrial and marine carbon sources. Marine carbon dates for the samples were calibrated using the Calib Marine98 and terrestrial samples were calibrated with Calib Intcal98 (Stuiver and Reimer, 1993). One marine sample was calibrated using the Fairbanks Calibration Program (Fairbanks et. al 2005) because the ^{14}C age date for that sample was beyond the limits of the Calib ^{14}C Calibration Program (Stuiver and Reimer, 1993).

3.4 Analog X-ray

The split cores that are at Lamont Doherty's curation facilities were scanned using an analog X-ray machine by the LDEO curatorial staff. The X-rays were shot at ~30cm intervals. The photographer allowed overlap between photos because in the process of taking the photos with the X-ray machine, the left and right ends become skewed. The darker areas of the X-ray images, which are less dense, can be interpreted as more clay-rich, and the lighter intervals as

more sandy. The analog X-ray images have aided in the identification of sedimentary structures that were not originally identifiable visually in the split cores. These sedimentary structures have helped with classification of paleo-depositional environments.

4.0 Results

4.1 Core Analyses

4.1.1 S4

Core S4 (Figure 8) sampled to a depth of 286.5 cm, close to the middle of the main channel in the mid-shelf study area (Figure 2b). The grain size is generally very fine to fine, with the exception of 3 intervals in the upper part of the core. The initial mean grain sizes sampled at depths ~25-45 cm range between ~1.2-2 phi (~435-250 µm). The average grain size shifts to ~3 phi (125 µm) around 48 cm. From this point until the bottom of the core, the mean grain size ranges between ~2.5-3 phi (~176-125 µm), with one small interval exhibiting a large grain size of ~1 phi (~500 µm), between 80-90 cm. Analog X-ray images of the S4 (Figure 8) core sections show mm- to cm-scale alternating laminations of darker and lighter bands throughout the core. The dark, presumably clay-rich bands (i.e ~118 cm in analog X-ray photo in Figure 8) are thicker in some intervals than in others, but never reach a thickness of more than a few centimeters. The clay rich band display lower density responses relative to the lighter sandier strata.

4.1.2 S5

Core S5 (Figure 9) sampled to a depth of 72.1cm, within the presumed fluvial infill near the SW edge of the main channel (Figure 2b). The initial mean grain size at the sampled interval, ~3-5cm, and the interval, ~13-16cm, is ~1.2

phi (435µm). In the section sampled, ~42-46cm, there is a slight increase in the mean grain size up to ~2.5 phi (~176µm). In the intervals sampled from ~54cm until the bottom of the core, the mean grain size values are clustered in a range ~2.8-3.1phi (~143-116µm). Analog X-ray of the S5 core displays a massive lighter deposit to a depth of ~65cm that sits unconformably on top of a slightly darker deposit with a slightly higher clay percentage.

4.1.3 S6

Core S6 (Figure 10) sampled to a depth of 335.6 cm in the middle of a presumed smaller tributary channel just to the SW of the main channel (Figure 2b). The sampled interval just below the surface down to ~45 cm depth exhibits mean grain sizes ~0.8-1phi (~574-500 µm). Just below 50 cm there are two sample points that show the mean grain size transitioning to larger phi values. From ~70 -100 cm, the mean grain size values are ~2.9-3.1 phi (~133-116 µm). This range is the approximate average range from the sampled intervals between 180 cm until the bottom of the core. There is one sampled interval around 175 cm that has a mean grain size of ~2 phi (~250 µm). The majority of the X-rays of core S6 show fine, thin, layered laminations that are cyclic, showing repetition in the depositional pattern. In a section of the S6 core from 200-230 cm (Figure 10) relatively flat-lying cycles of fine laminations occur. At ~215 cm, the flat-lying stratigraphy first develops a concave-down geometry and then becomes relatively flat at ~210 cm. Also at this point, the darker, more clay- rich layering

within the laminations become thicker. In the interval of 210-200 cm, there is a relatively massive deposit, followed by a ~1-2 cm size band of a darker layer, that has a concave up geometry and appears to be truncating the massive, lighter colored layer beneath.

4.1.4 S19

Core S19 (Figure 11) sampled to a depth of 579 cm, near the NE edge of the main channel (Figure 2b). The initial intervals sampled contain mean grain sizes values of ~1-2.1 phi (~500-233 µm). Below 100 cm, the mean grain sizes are ~3.1-3.5 phi (~116-88 µm) in various sampled intervals down to ~450 cm. At ~490 cm, the mean grain size increases to ~6.8-9 phi (~9-2 µm) within the sampled intervals. The analog X-ray of S19 core also shows alternating mm-scale laminations of darker and lighter strata throughout the core. Near the base of the core, the darker strata reach a thickness of ~10 cm (Figure 11).

Nine ^{14}C dates were acquired from S19 core, eight bulk carbon on muds at various depths and one from a shelf fragment at 490cm (Table 1). The radiocarbon ages from the bulk carbon analysis of the muds are quite consistent in the range 10,975-11,445 ^{14}C age years BP. Assuming a marine source, these dates calibrate to 12,586-13,027 years BP. Assuming a terrestrial source, these dates calibrate to 12,864-13,355 years BP. The δ13 values (Table 1) for the bulk carbon samples are $^{-}22.5$-$^{-}26.7$ $^{o}/_{oo}$, which indicates a mixed carbon source within this channel, thus the true age probably lies somewhere between the two end

members. The radiocarbon date from the shell fragment is considerably younger than the bulk carbon dates: a marine calibrated age of 10,247 +- 90 years BP.

4.1.4 S20

Core S20 (Figure 12) sampled to a depth of 236 cm and penetrated the interfluve/ stiff clay that separates the two observed incisions in the mid-shelf system (Figure 2b). The core has initial mean grain sizes just below the surface of ~.8 phi (~574 µm), with a mean grain size of ~7-10 phi (~8-1 µm) within the same interval and just below at ~50cm. Around 90-100cm, as well as the sampled interval just below 200 cm, the mean grain sizes are ~2.8-3.2 phi (~143-108 µm).

Analog X-ray images of this core (Figure 12) did not reveal any sedimentary structures. There was one reliable ^{14}C date (Table 1) at the bottom in some carbonate mud of 35,430 +- 686 ^{14}C years BP. The marine calibrated age for this mud is 40,734 +/- 686 years BP.

4.1.5 162_02B

Core 162_02B (Figure 13), which was taken in the outer shelf channel (Figure 2a), sampled to a depth of 206.5 cm. The sampled interval from 0-50 cm exhibits mean grain sizes ~1.2- 1.6 phi (~435-329 µm). Below this interval, the samples from the interval 50-100 cm have mean grain sizes between ~8.1-9.1 phi (~3.6-1.8 µm). There is a decrease in the mean grain size over 100-150 cm

from ~5 phi to 7.2 phi (~31 to7µm). Below this interval to the bottom of the core, the sampled intervals have a mean grain size of ~7.2 phi (~7µm).

The analogy X-ray image for core 162-02B (Figure 1) showed very little by way of sedimentary structures. There are, however, lenses that may be burrow structures, which are mostly filled with sand (Figure 13), and thin sand stringers within the clay rich massive strata. We have not yet obtained the ^{14}C results from the mud within this core. However, there have been dates acquired from cores that were sampled in channel fill sediments at similar depths in previous studies. These include an age of 12,500 years BP reported by Buck et al. (1999) and an age range of 13,590-15,600 years BP reported by Christensen et al. (2000) (Table 2).

4.1.6 S11

Core S11 (Figure 6) sampled to a depth of 200cm. This core was not sampled for grain size analysis but it was sampled for ^{14}C dating. However, this core is important because it penetrated ~2m of shelly Holocene sand before bottoming out in the T horizon (Figure 6). Shell material was taken for ^{14}C analysis and the ^{14}C age date is 9,555 years BP. The marine calibrated age range is 10,337-10,506 years BP (Table 1).

4.2 Foraminiferal Analysis

A qualitative foraminiferal analysis of the coarse fraction was performed by Christensen (unpubl. data). intervals revealed the occurrence of the benthic foraminifera genera *Elphidium*. *Elphidium spp.* reflects a marine environment with water depths between ~ 20-40 m waters depth. The associated assemblage that *Elphidium spp*. can be found within, could record a regressive tendency within a shallow marine environment that has a progressive increase of freshwater influence (Amorosi et al., 2007).

Elphidium spp. was found in samples from the S5 core in the mid-shelf channel (Figure 2b) and the outer shelf channel core 162_02B (Figure 2a). *Elphidium spp.,* when found alone and not as a part of an assemblage, does not reveal the depositional environment, but *Elphidium spp.* was found as part of an inner-to-middle shelf assemblage (~10-40m water depth) during cluster analysis of another outer shelf core in channel fill (Buck et al. 1999) and this core location is near the location of the outer shelf channel in my study area. The occurrence of *Elphidium spp.* within the assemblage of *Ammonia spp.* and/or *Trachimina spp.* (other benthic foraminifera*)* can be indicative of a shallow marine estuarine environment, but we have not been able to verify this assemblage in our core data, as *Ammonia spp.* and *Trachimina spp* were not present.

5.0 Discussion

5.1 Age Constraints on mid-shelf channel infill

Previous studies (Davies et al. 1992, Buck et al. 1999; Duncan 2000; Christensen et al., 2007, and many others) have attempted to constrain the timing of infilling of the outer shelf, but no constraints have been placed on the mid-shelf channel infilling. However the timing of deposition within the mid-shelf channel can be constrained by ^{14}C ages dates obtained from samples taken as part of this study. Wright et al. (2009) have recently proposed a sea-level curve for the New Jersey shelf. Correlation my ^{14}C dates and the reconstruction of paleodepths from this study with that sea-level curve, in association with the channel depth ranges, allows for a conceptual understanding of the timing of the deposition on the mid-shelf as well as on the outer shelf (Figure 14 a-d).

The interfluve, the horizontal to sub-horizontal reflectors that separate the main channel from the smaller tributary channel (Figure 2b) was sampled by the S20 core. These sediments presumably represent pre-existing sediments that were eroded by the fluvial channels during the subaerial exposure associated with the LGM. The sample at ~156 cm has a calibrated age date of 40,734 +/- 686 years BP (Table 1). In contrast both marine and terrestrial bulk carbon dates acquired from the mud within the channel in core 19 at depths of ~45-576 cm, revealed an age range of ~12,500-13,500 years BP (Table 1), much younger than the age of the interfluves sediments, as expected. However, this age range of fill, based on the sea-level curve, as well as sea level proximity during infill, is

slightly older than expected age range (Figure 14a). As shown in Figure 14a, the channels in the mid-shelf system have a range of ~35-40 m. The expected age for deposition within the channel according to the sea-level curve would be ~10-11 ka. It is also nearly 2000 years older than the radiocarbon age of the shell fragment found at 490 cm within core S19 (Figure 2b). It is significant to note the difference in the shell and mud ages with the mid-shelf channel, because this is likely due to re-deposition of the sediment within the channel. The consistency of the bulk carbon age dates provides confidence in the dating method, but the radiocarbon ages (~12,500-13,500 y BP) may not be the actual ages of deposition. To reconcile the age discrepancy between bulk carbon and shell ages in core s19, I suggest that the bulk carbon ages obtained from these samples are from reworked sediment. Therefore, the ^{14}C age dates that were acquired record their original deposition age. They were possibly brought down onto the shelf from an upstream location of marine or terrestrial origin. This leads me to infer that the timing of the sediment infill may in fact be younger than the dates obtained and constraining infill timing can be performed more consistently with shell material found in core S19.

Figure 14b shows the New Jersey sea-level curve and the marine carbon calibrated ^{14}C dates from the shell material found in the mid-shelf channel from cores S11 and S19, along with the channel depth ranges for the mid-shelf. The shell material within the mid-shelf channel (S19) has a calibrated age of 10,247 +- 90 years BP. S11 bottoms out in the T-horizon (see Figure 6), the interpreted

transgressive ravinement surface (Duncan 2001), which must be stratigraphically younger than the mid-shelf channel fill sediment. The calibrated age date for the shell material found within the T-horizon is 10,421 +- 66 years BP. The possibility of reworking is virtually certain for the shell material at the ravinement surface, but the age dates are both consistent with the position of sea level being at or near these depths at these times (Figure 14b). The S11 shell date from within the T-horizon (Figure 6), which transgresses the mid-shelf channel, shows a slightly older ^{14}C age date (10,421 +- 66 years BP) (Table 1) than the shell material within the mid-shelf channel. However, S11 is located in slightly deeper waters (~40-45 m) to the southeast of the mid-shelf channel system (Figure 1b). The difference in the two ages possibly helps mark the timing of transgression of the channel, as the S11 area must have been transgressed prior to the mid-shelf channel system during very late stages of the Pleistocene into the very early stages of the Holocene.

Based on the ^{14}C radiocarbon dates acquired from the mid-shelf channel and through correlation with the New Jersey sea-level curve (Wright et al. 2009), the mid-shelf infill sediments were likely deposited very proximal to the shoreline. The S11 T-horizon shell (Figure 6) and the S19 channel fill shell are very close in age (Table 1). The presence of the benthic foraminifera *Elphidium,* which was found in inner-to-middle shelf assemblage (~10-40m water depth) during cluster analysis of another outer shelf core in channel fill (Buck et al. 1999), also

supports the inference that the mid-shelf channel infill was proximal to the shoreline.

5.2 Depositional environment of mid-shelf channel infill

Some evidence for the depositional history within the mid-shelf channel can be deduced through a section of the S6 core (Figure 2b). If the deposition was similar to the (Zaitlin et al. 2004) estuarine model, I would expect to have seen a fluvial succession within the S6 core, followed by estuarine sedimentation, perhaps fining upward sequences with large grain sizes near their bases. The S6 core appears to have some wave and/or tidal influence sedimentological features over 200-230 cm (Figure 15), confirming an estuarine influence. From ~230 cm to ~220 cm, the stratigraphy is relatively flat lying with thin layering. I suggest that deposition within this interval was therefore below the wave base and accommodation was possibly increasing. Just above ~220 cm, there appears to be a hummocky feature (Figure 15) that is suggestive of wave and/or tidal influence during deposition. Also, between 220 cm and 210 cm one stratum appears to truncate the underlying strata (Figure 15). This could be indicative of a system that is keeping up with sea level as a dense, perhaps hyperpycnal tidal flow, erodes underlying material as it enters the system. Sedimentary structures such as hummocks record the wave and tidal influence as the accommodation is limited. The deposit with an erosive base suggests that the flow was rapid and dense. This is important, because the seismic

stratigraphy of the mid-shelf channel (Figure 2b) shows U-shaped geometries that I interpret as repeated episodes of down-cutting in a high energy environment (Duncan, 2001). Throughout the entire 200-230 cm interval, there is an overall imprint of increasing accommodation, perhaps indicative of continuously rising base sea level, because the darker strata are increasing in thickness upward, while the lighter strata also slightly increase in thickness (note the massive lighter strata just below the truncation feature in Figure 15). The massive lighter strata also show some possible deformation, perhaps due to rapid sedimentation (on Figure 15).

I am going to explore the hypothesis that the mid-shelf sediments are derived from the catastrophic meltwater flood deposits as proposed by previous studies Donnelly et al. (2005) and Thieler et al. (2007). The timing of the melt-water flood event is consistent with the radiocarbon age constraints for sediment that was possibly transported through the glacial outwash from the north. The sedimentology in the systems is also consistent because the grain size data within the mid-shelf channel (Figures 8-13) indicate sizes that typically range between very fine and fine sand. The stratigraphy displays geometries consistent with sediments that were possibly under wave and/or tidal condition as deposition took place within the channel. The high width to depth ratio is similar to the cross sectional morphology of suspended load, terrestrial river channels. (Schumm, 1985; Galloway and Hobday, 1996; Blum and Tornqvist, 2000; Duncan, 2001).

The seismic stratigraphy in the mid-shelf channel (Figure 2b) displays geometries that are quite different than the geometries in the outer shelf channel (Figure 2a). The difference in the geometries could be because the outer shelf channel was back filled due to transgression, while the mid-shelf channel was filled during a catastrophic meltwater event (Thieler et al., 2007) (Figure 5) from the north. The timing for the catastrophic meltwater event is also generally consistent with the age dates found in the mid-shelf channel (Table 1). Figure 16 shows the time constraints of the meltwater flood event. The ^{14}C age dates from the mid-shelf channel system fall within those constraints, which leads me to infer that the sediment infill within the mid-shelf channel could have deposited on the mid-shelf during the flood event and re-deposited in the mid-shelf channel ~10-12,000 ka. This would also explain the sedimentological evidence for the deformation in the fill.

I suggest that the glacial meltwaters that were redirected to the south, as well as the glacial meltwaters waters that breached the banks of the HSV to the south, could have incised and/or flooded the exposed shelf and continued to flow to the south and southeast. This hypothesis is shared by Uchupi et al., (2001) and Duncan (2000), who have suggested that the water that drained through the Long Island terminal moraine may have carved the channel system and provided the infill sediment in the mid shelf channel system.

The catastrophic meltwater flood event likely supplied the entire continental shelf with a large volume of sediment. In the mid-shelf, the large

volume of sediment that did not get localized by the HSV could have localized within the mid-shelf channel system. On the mid-shelf, after flooding, passive infilling of the river drainage system with finer-grained fluvial sediment is the dominant process until the channels are transgressed (Wood and Hopkins, 1989). This passive infilling is eventually accompanied by tidal influxes as sea-level rises. Infill sediments are then deposited in both landward and seaward directions causing such features as the possible hummocky structure seen in Figure 15. The cohesive sediments moving back and forth with the tides maintained the basal shape, producing the U-shaped reflections now observed (Figure 2b).

5.3 Age constraints on outer shelf channel infill

The outer shelf channel system within my study area has been previously sampled for ^{14}C in an effort to constrain the timing of infill. Buck et al. (1999) and Christensen et al. (2007) both sampled cores near the outer shelf channel mapped and interpreted by Nordfjord et al. (2006). (Figure 3) Buck et al. (1999) used previously published AMS ^{14}C dates from Lagoe et al. (1997), which placed the infilling of the outer shelf channel at ~14,464 years BP (uncalibrated 12,500 ^{14}C years BP) (Table 2). Wood and shell fragments were both used by Christensen et al. (2007) during the radiocarbon age dating process (Table 2). They found age dates 12,285-13,542 ^{14}C years BP (which calibrated to calendar ages 13,590-15,600 years BP). These two data sets are fairly consistent, with

deposition being within an estuarine environment (Figure 14c). The relative timing of the infilling of the outer shelf channel systems on the New Jersey shelf must have occurred prior to the infill of the mid-shelf channel, as the Holocene transgression of the shelf is more or less continuous (Wright et al., 2009), so our data confirms that the outer shelf was transgressed prior to the transgression of the mid-shelf system. The outer shelf transgression appears to have occurred ~12, 000-13,000 years BP and the transgression of the mid-shelf channel occurred ~10,000 years BP or shortly thereafter (Figure 14d).

5.4 Depositional environment of outer shelf channel infill

The seismic stratigraphy of the outer shelf channel (Figure 2a) has been interpreted by Nordfjord et al. (2006, who mapped these NW-SE trending dendritic channel systems (Figure 3b) and interpreted the facies superposition in the mapped valley fill that is partly consistent with a model of wave-dominated estuaries (Dalrymple et al., 1992; Zaitlin et al., 1994; Figure 4). The segment III bayhead delta is poorly developed, possibly because of low sediment discharge. Also, the hightstand systems tract does not occur, but the wave ravinement surface is present. In their interpretation, they found an ordered sequence suggesting a transgressed fluvial/estuarine system: (1) fluvial lag deposits, (2) central bay muds, and (3) barrier sands, all of which are overlain by the Holocene sand sheet. Core 162_02B, which sampled to a depth of 206.5 cm in this filled

channel, was able to penetrate layers that I interpreted as central bay muds that are overlain by barrier sands (Figure 17).

The fine-grained sediments below 50 cm in core 162_02B are consistent with the central bay mud interpretation of Nordfjord et al. (2006) for this unit. The fine-grained silty mud is very stiff and indicative of the low energy depositional environment of this estuarine system at that time. The medium sands in the interval 0-50 cm could be interpreted as barrier sands. However, the presence of mud in these sands is problematic to this interpretation. Barrier sands are deposited in a very energetic environment (Dalrymple et al., 1992). Hence, finer grained material should have been winnowed out. Therefore, I suggest that the interval sampled above 50 cm in this study is the transition zone from the low to high energy environment and the homogenous barrier sand has not been sampled by Core 162_02B.

5.5 New Jersey mid-shelf channel fill depositional model

The majority of the research on the latest Pleistocene-Holocene sedimentation across the New Jersey shelf focuses on sedimentation during the latest sea-level transgression in terms of a basic estuarine model. The fluvial systems were established on the shelf as the Laurentide Ice Sheet advanced to its terminal moraine position (Figure 5). The sea-level rise after the LGM caused deposition to occur within the channel as it was back-filled as the shelf was transgressed. Using this scenario, I have tried to place the mid-shelf and outer

shelf channels into the same depositional model. The mid-shelf channel system would have been the equivalent of segment III and the outer shelf channel system would have been the equivalent of segment II of the Zaitlin et al. (1994) incised valley model (Figure 4). The outer shelf channel system mapped and interpreted by Nordfjord et al. (2006) displays the necessary characteristics to be the segment II within a depositional model because of the presence of the fluvial lag deposits, central bay muds, and barrier sands, all of which are overlain by the Holocene sand sheet. However, the mid-shelf channel does not appear to be completely equivalent to segment III. Based on the sea-level curve and the radiocarbon age dates within the mid-shelf channel, infilling of the mid-shelf channel occurred proximal to the shoreline.

6.0 Conclusion

This study aided in the ground-truthing of seismic work previously done on the New Jersey shelf and provided new information on the mid-shelf channel system. The ground-truthing of the outer shelf channel was partly achieved by the identification of the central basin mud through grain size analysis. The carbon source for the mud in the sampled system is not completely understood, but based on the δ13 values of ¯22.6-¯25 o/oo from this study, the sampled mud appears to have both has both a marine carbon source and a terrestrial source, leading me to infer a likely estuarine environment within the mid-shelf channel.

From this study, the end of mid-shelf channel infilling can be better constrained around ~10 ka, which is after infilling of the outer shelf channel at ~ 14 ka. The mid-shelf channel system infilled very close to sea level, as some analogy X-ray images displayed evidence of wave and tidal dominance. Foraminiferal data revealed the presence of *Elphidium spp.* which is abundant (e.g. Poag, 1981) in a shallow marine estuarine environment. The calibrated ^{14}C age dates are consistent with the sea-level curve as the re-depositional ages of the mid-shelf sediment are ~12 ka. The infilling of the mid-shelf channel could also possibly be the result of a catastrophic meltwater flood event that occurred during the latest stages of the Pleistocene. The flood event possibly supplied the mid-shelf with a large volume of sediment that was re-deposited proximal to the shoreline during a relative sea-level rise ~10-12 ka. Available ^{14}C ages from the mid-shelf and outer-shelf channel fill sediments, in comparison with a recently

published New Jersey shelf sea-level curve, show that the time of infilling of the mid- and outer shelf was during a relative sea-level rise, and that the depth of deposition was at or slightly above sea level for the mid-shelf channel system. This result is consistent with deposition in an estuarine environment. Based on grain size analysis, as well as density log data, we find that the mid-shelf channel is sandier than the outer-shelf channel. This leads me to infer that the sediments from the mid-shelf channel were deposited in a higher energy environment than that of the sediments in the outer shelf channel.

The geometries of the seismic reflectors also provide evidence for the nature of deposition. In the mid-shelf channels, the U-shaped reflectors are possible indicators of tide process within the channel during deposition. The cut-and-fill geometry is likely associated with a higher energy depositional environment relative to the outer shelf channel system. The outer shelf channel system displays more flat lying reflectors that are likely associated with a lower energy depositional environment.

Further research on the New Jersey shelf must be done. Detailed mapping of the mid-shelf would provide a better understanding of the morphology of the mid-shelf channels and their drainage directions. Also, deeper cores within the mid-shelf channel targeted in this study that penetrate to the incised substrate and channel flanks would provide a better depositional history. Deeper cores in the outer shelf channel in areas that possibly display the entire estuarine sequence interpreted by Nordfjord et al. (2006) would further aid in the

groundtruthing of their seismic work. As these techniques are further implemented, the understanding of the latest Pleistocene-Holocene stratigraphy of the New Jersey shelf will also improve.

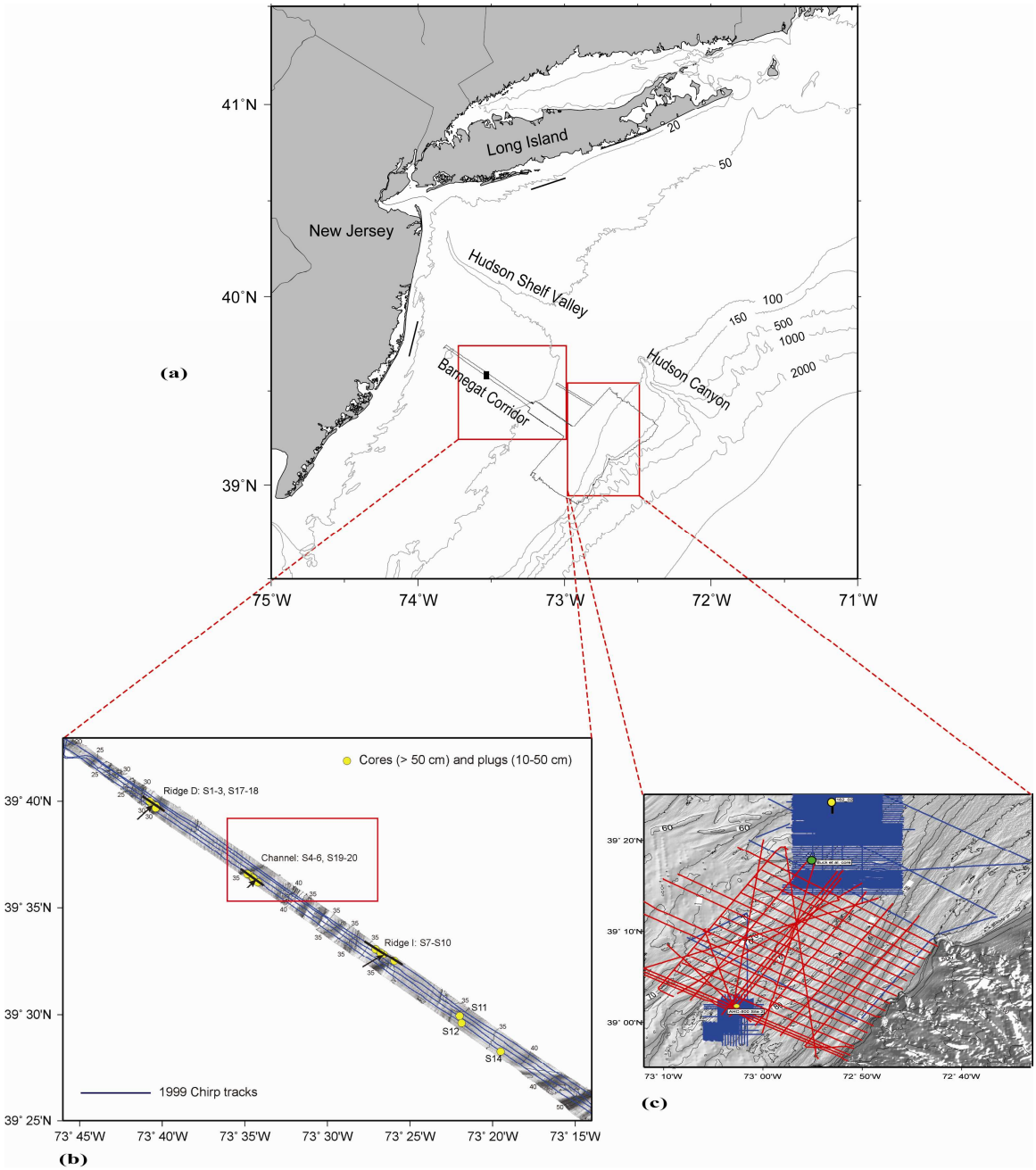

Figure 1: **(a)** Map of study area from KN190 cruise report of the Barnegat Inlet along the Barnegat Corridor, New Jersey shelf with boxes outlining local study areas. **(b)** Map from KN190 cruise report of vibracores collected within the Barnegat Corridor. Bathymetric map with contours in meters and artificial illumination from the north, from existing multibeam data. CHIRP seismic reflection track lines from Duncan (2001). Red box indicates location of inner shelf channel (shown on Figure (a) with black square). **(c)** Bathymetry of outer shelf area with contours in meters and artificial illumination from the north, from existing multibeam and artifact data. Blue lines represent chirp seismic track lines from Nordjford et al. (2006) and red lines represent CHIRP seismic data from KN190 cruises (2007). The yellow dot represents location of outer shelf core 162_02. Green dot represents location of the Buck core et al. (1999).

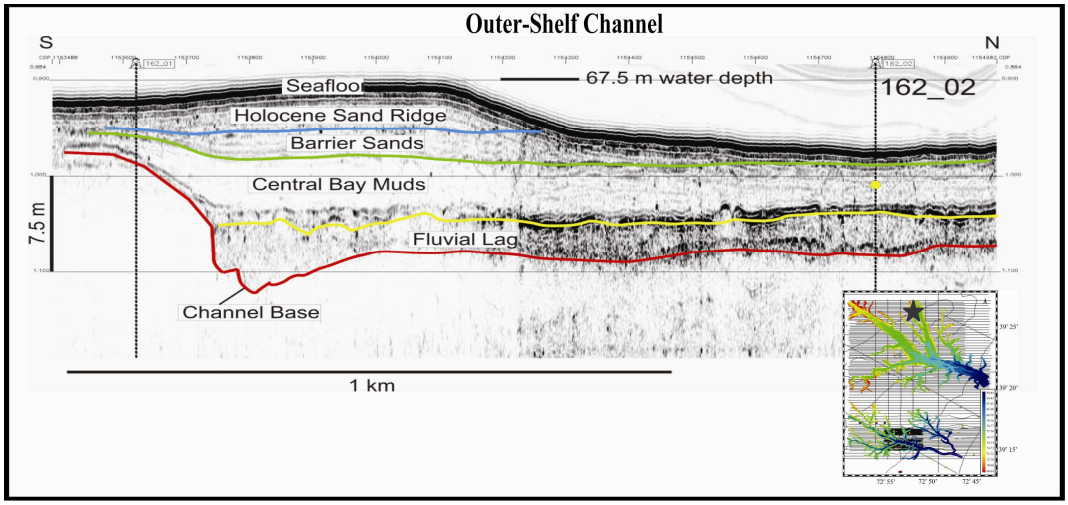

Figure 2a: Stratigraphy of the outer-shelf channel that is positioned currently in ~70-80 meters water depth. Flat lying reflectors have been interpreted by Nordfjord et al. (2006) as a well ordered sequence with identifiable reflectors. Also includes map of outer-shelf channel system interpreted by Nordfjord et al. (2006), black star showing the position of the outer-shelf channel. Location of core 162_02, discussed in the text, is also shown. VE = ~25x

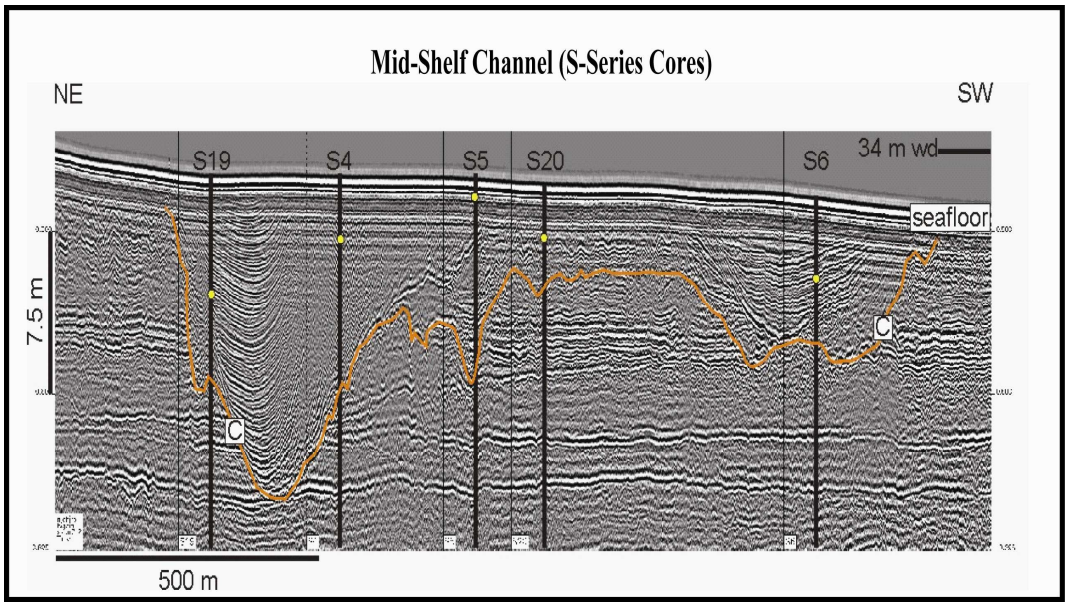

Figure 2b: Stratigraphy of the mid-shelf channel and a presumed tributary (to the right) that is positioned currently in ~35-40 meters of water depth. The U-shaped geometries of the reflectors are noticeably different from the relatively flat lying reflectors in the deeper water channel system (Fig. 2a). Yellow dots represent depth of penetration. Location of this profile is shown in Fig. 1a. VE = ~42x

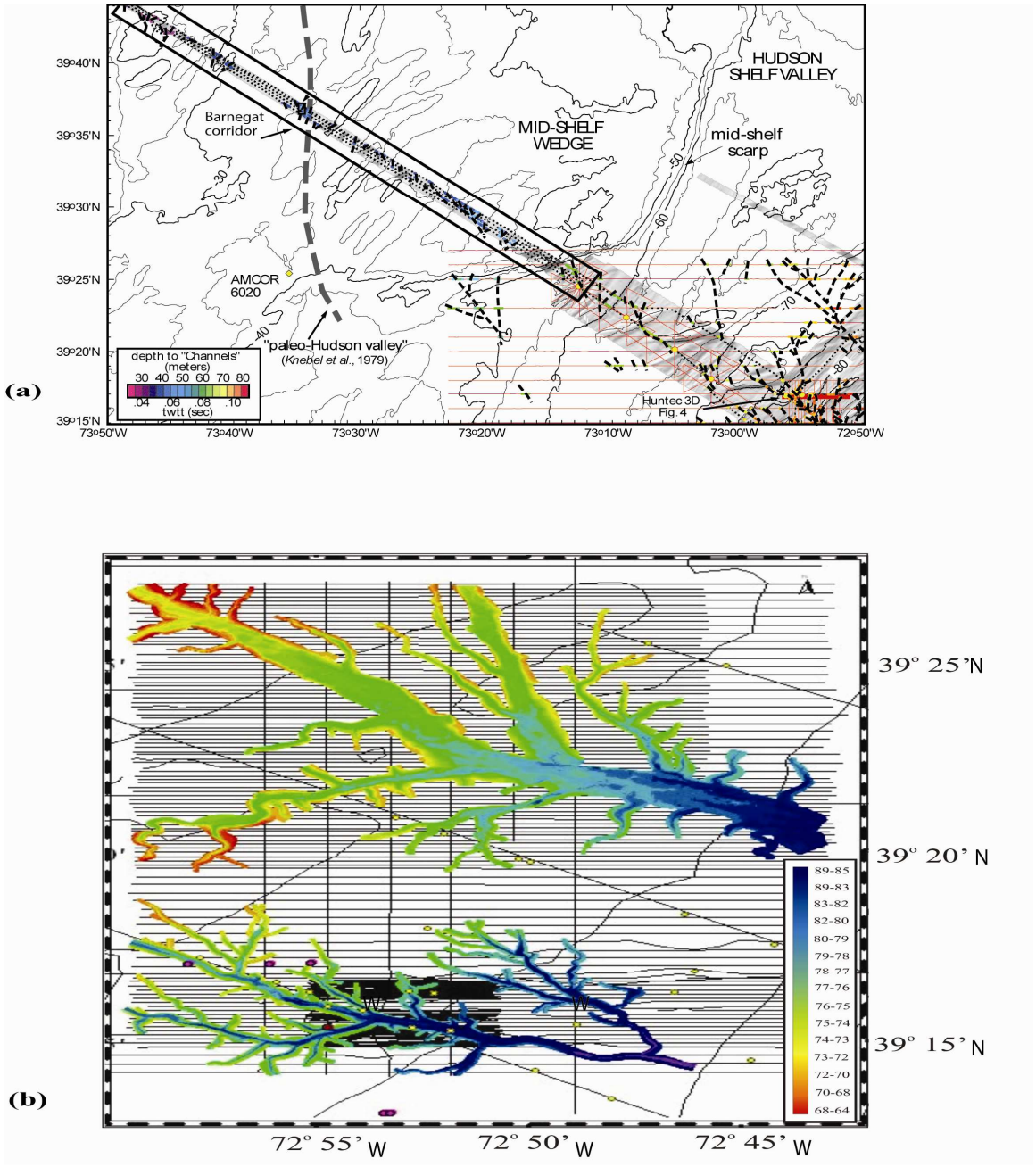

Figure 3: Map of the mid-shelf and outer shelf channel system. **(a)** Map of S-series channel horizons across the inner and middle shelf from Duncan (2001). Yellow lines are chirp sonar profiles and red lines are 2D/3D Huntec reflection record. Red lines and boxes from Austin et al (1996) and Duncan et al (2000). Yellow dots are from 1993 vibracore sites (Davies et al., 1997; Lagoe et al., 1997; Buck et al., 1999) and yellow dots are from an AMCOR site (Hathaway et al., 1976; Sheridan et al., 2000). **(b)** Dendritic channel system mapped by Nordjford et al. (2006). Black lines represent chirp seismic track lines from 2001, which were used to construct the map.

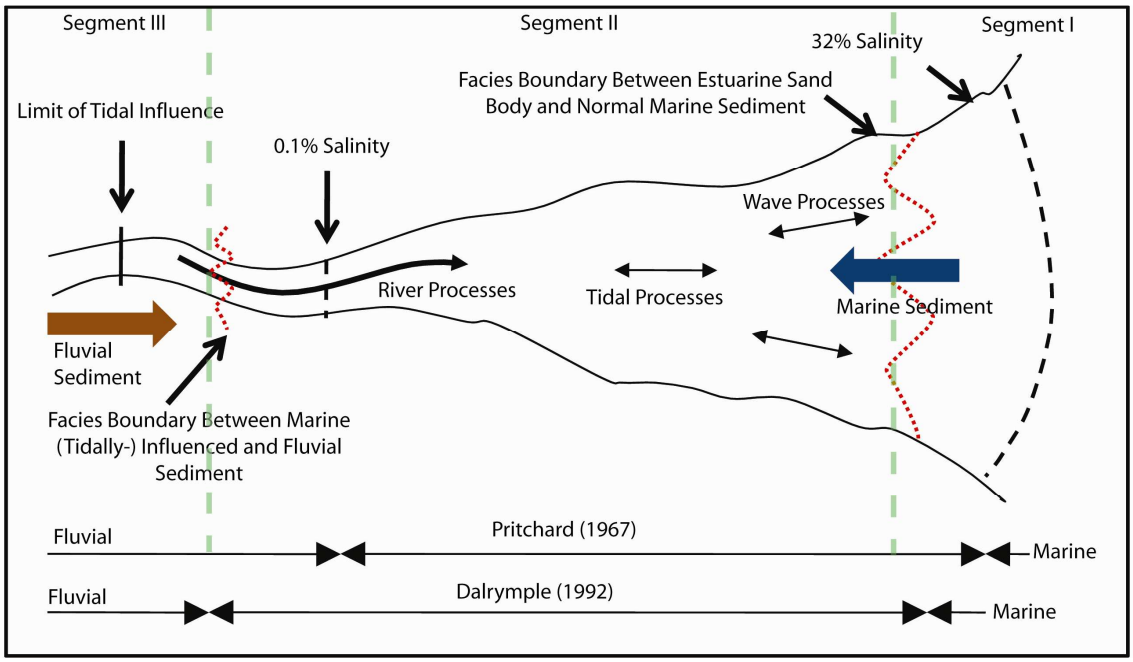

Figure 4: Schematic diagram showing variations in definition of estuary. Pritchard (1967) limits defined by salinity and Dalrymple et al. (1992) limits defined by facies boundaries and transgressive character. Green dashed lines define limits of incised valley segments defined by Zaitlin et al. (1994).

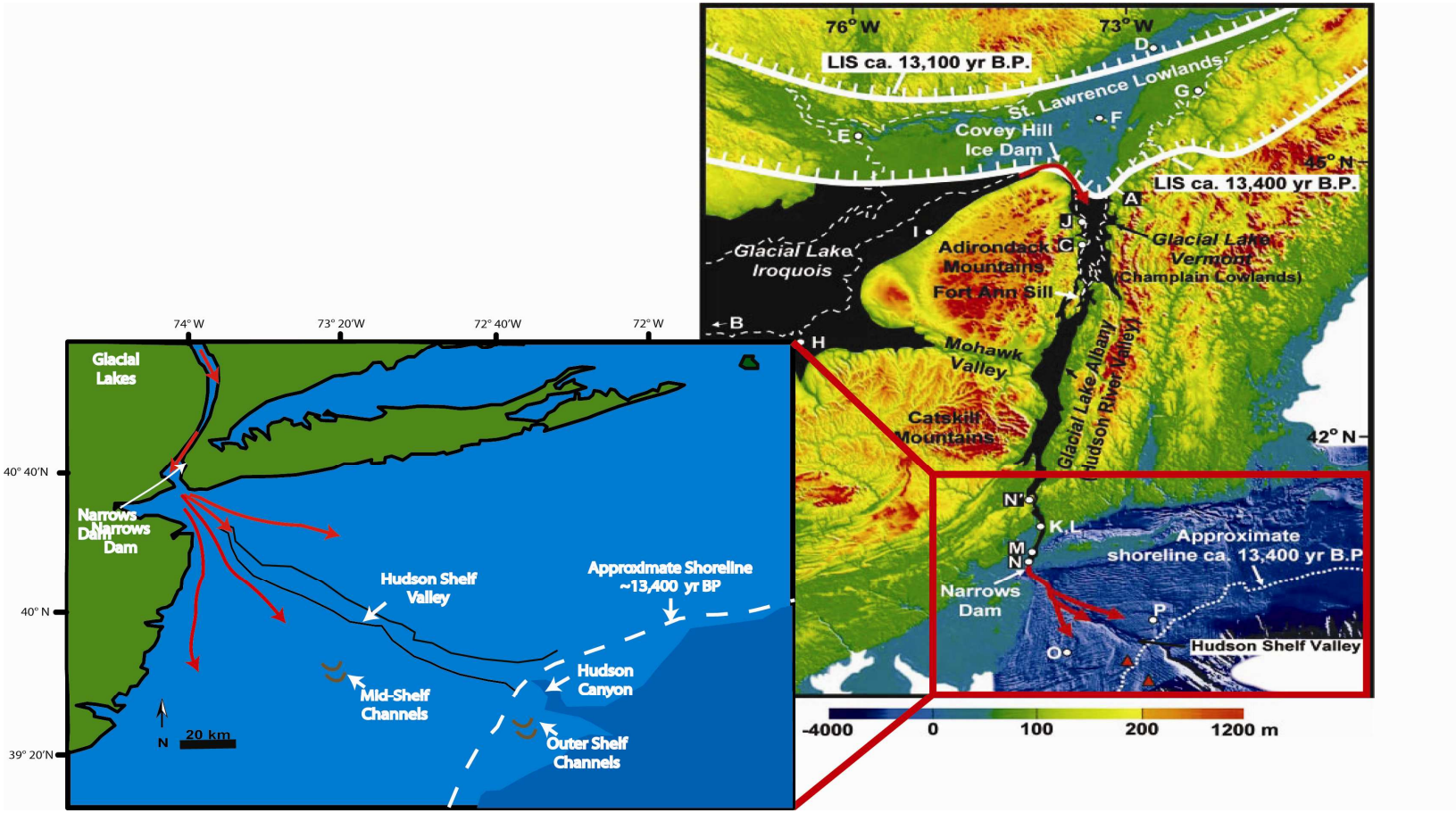

Figure 5: Photo (right) from Donnelly et al., (2005) showing positions of glacial lakes and route of discharged glacial meltwaters. Schematic diagram (left) showing routes as meltwaters from glacial lakes to the north breached the Narrows and disbursed onto the New Jersey shelf. White dash line shows approximate shoreline ~13,400 years BP.

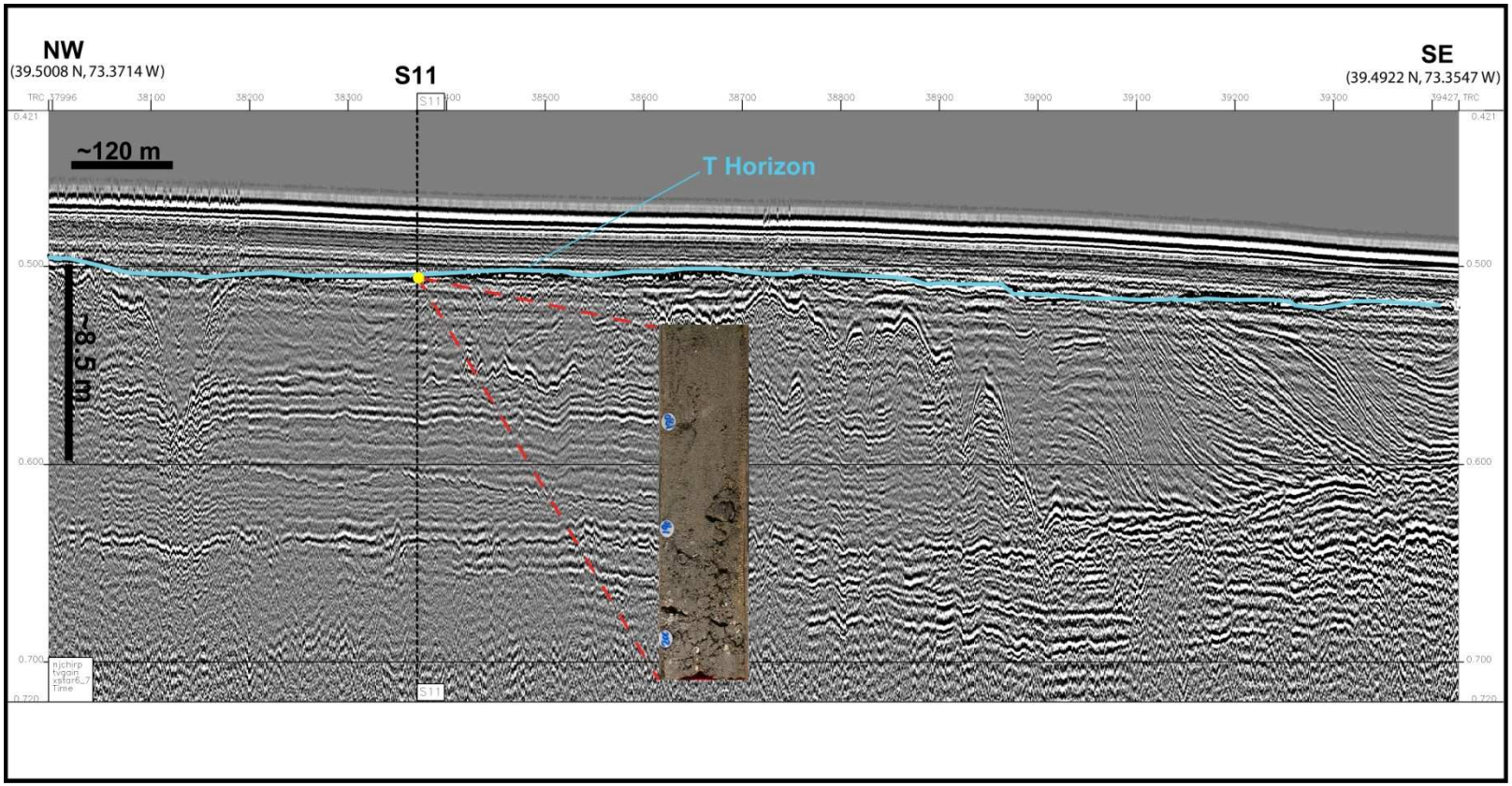

Figure 6: Stratigraphy along mid-shelf that was penetrated by core S11. Core photo showing sediments that were penetrated. T-Horizon denoted by the blue line and lies at the base of the core photo. Yellow dot represents depth of penetration. VE = ~26x

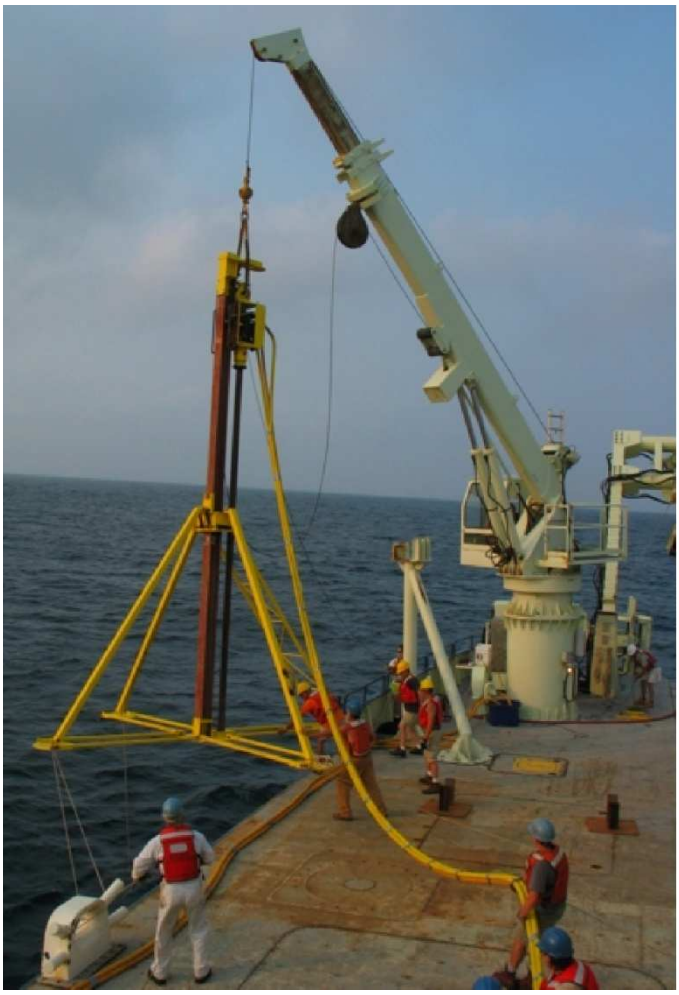

Figure 7: Photo of 20ft vibracore configuration from Kn190 cruise aboard the *R/V Knorr* during the summer of 2007.

Radiocarbon dates from mid-shelf

Sampled Depth (cm)	d13 values	14C Age (y BP)	Calibrated Marine 14C age (y BP)		Calibrated Terrestrial 14C age (y BP)		Age Uncertainty (years)
			Start	End	Start	End	
S19 -(45-56)	-25	11338	12852	12918	13161	13269	60
S19 -(120-121)	-23.9	11044	12637	12807	12637	12807	72
S19 -(142-143)	-24.2	10975	12586	12750	12864	12947	60
S19 -(259-260)	-22.5	11130	12738	12833	12965	13092	60
S19 -(300-301)	-22.9	11271	12828	12883	13110	13216	60
S19 -(400-401)	-23.1	11113	12723	12823	12957	13080	60
S19 -(440-442)	-22.7	11145	12756	12841	12972	13104	59
+ S19 -(490)	n/a	9389	10157	10338			79
S19 -(575-576)	-22.6	11445	12901	13027	13241	13355	63
*S20 -(156-159)	-26.7	35430	40735 +/- 686				
+#S11 -(200)	-0.5	9555	10337	10506			66

+ denotes shell material, all others are bulk carbon from mud samples

* denote calibration done using Fairbanks (2005), others calibrations performed with CALIB (Stuiver and Reimer, 1993), S20 penetrated interfluve/stiff clay Pleistocene substrate.

S11 did not sample mid shelf channel, but did penetrate the transgressive ravinement surface.

Table 1: Table showing sampled intervals with associated ages from ^{14}C dating by Arizona State University.

Radiocarbon dates from outer shelf

Sample Depth (mbsf)	Material	D13 values	14C Age (y BP)	Calibrated Age	Age Uncertainty (years)	Calibration Method
Christensen et al., (2007)						
0.99	Shell	-0.45	12565	13590	41	Marine98
0.00-1.62	Wood	-27.45	12974	15600	43	Intcal98
0.60-3.00	Wood	-28.20	12346	14270	45	Intcal98
2.95	Wood	-27.03	12294	14250	44	Intcal98
4.28	Shell	-0.67	13522	15000	42	Marine98
5.28	Wood	-28.18	12285	14240	45	Intcal98
6.37	Shell	-1.66	13417	14880	46	Marine98
10.81	Shell	-0.93	13542	15020	62	Marine98
Buck et al., (1999)			12500	14464		Fairbanks

Table 2: Table showing sampled intervals with associated values from ^{14}C dating from Buck et al., (1999) and Christensen et al., (2007). Buck et al. dates, calibrated using Fairbanks Calibration Program (Fairbanks et. al 2005). Christensen et al. dates, calibrated using CALIB 4.4 (Stuiver and Reimer, 1993).

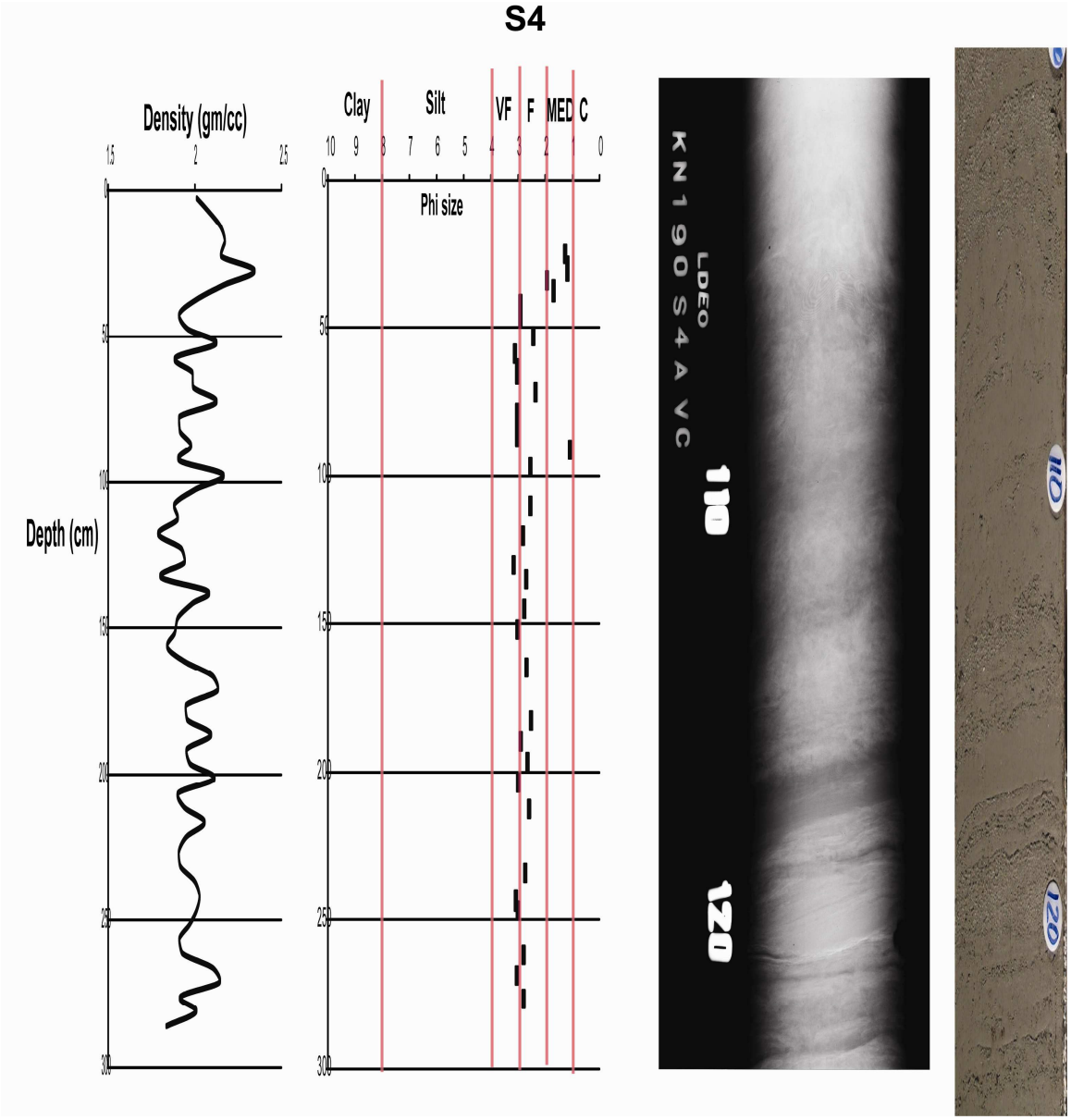

Figure 8: Graph (left) showing bulk density (gm/cc) versus depth (cm), alongside grain size (φ) versus depth (cm) for core S4 (see Figure 2b for location). Bulk density was acquired aboard the *R/V Knorr* as cores were brought onboard during the 2007 cruise. Black dots represent sampled intervals. VF= very fine, F = fine, MED = medium, C= coarse. Analog X-ray image (right) and photo of segment of core S4 provided by Lamont Doherty core facility. Analog X-rays showing mm to cm scale, alternating lamination of darker and lighter bands.

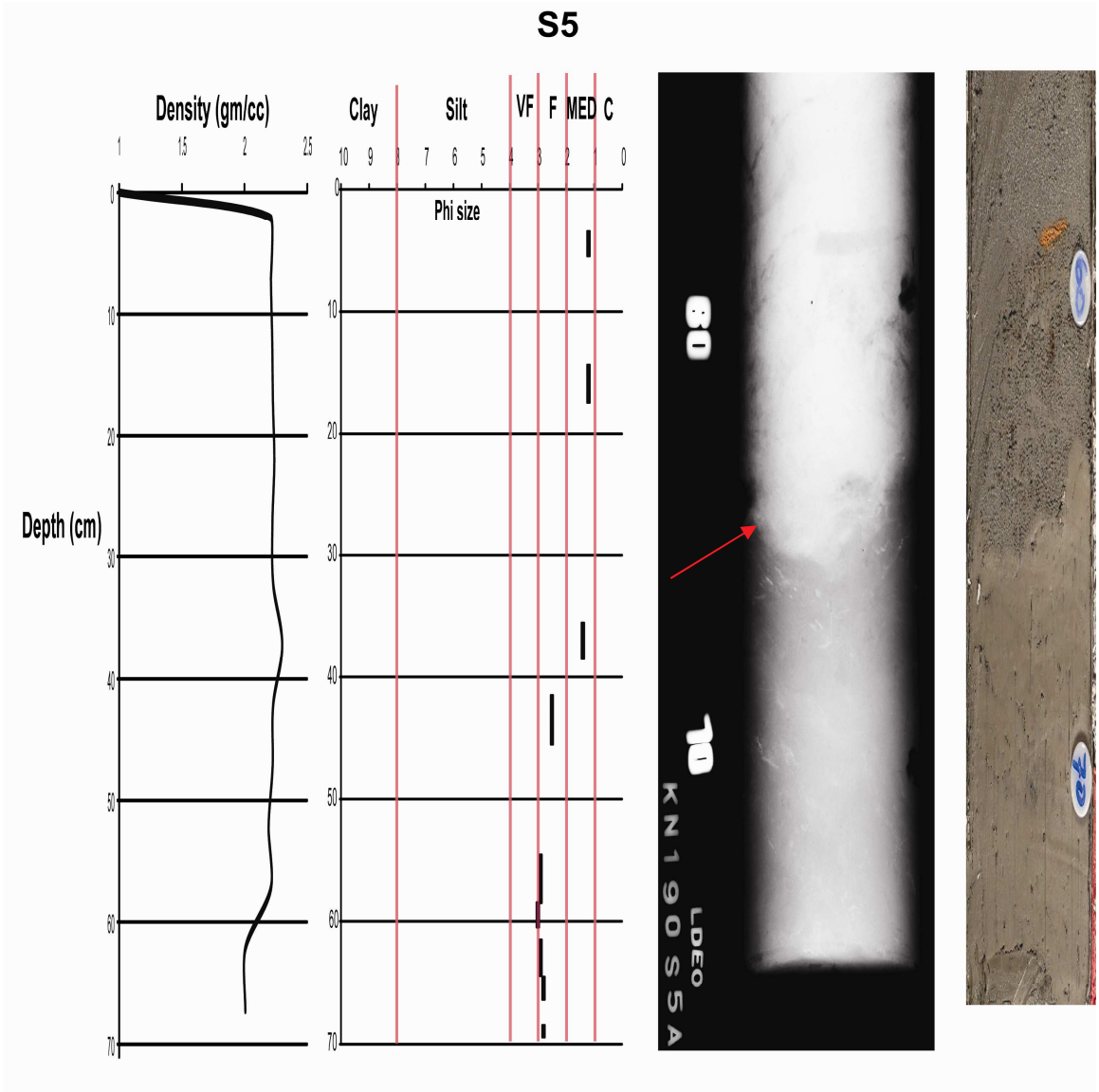

Figure 9: Graph (left) showing bulk density (gm/cc) versus depth (cm), alongside grain size (φ) versus depth (cm) for core S5 (see Figure 2b for location). Bulk density was acquired aboard the *R/V Knorr* as cores were brought onboard during the 2007 cruise. Black dots represent sampled intervals. VF= very fine, F = fine, MED = medium, C= coarse. Analog X-ray image (right) and photo of segment of core S5 provided by Lamont Doherty core facility. Analog X-rays showing massive lighter deposit to depth of ~65cm sitting unconformably atop a slightly darker deposit, denoted by red arrow.

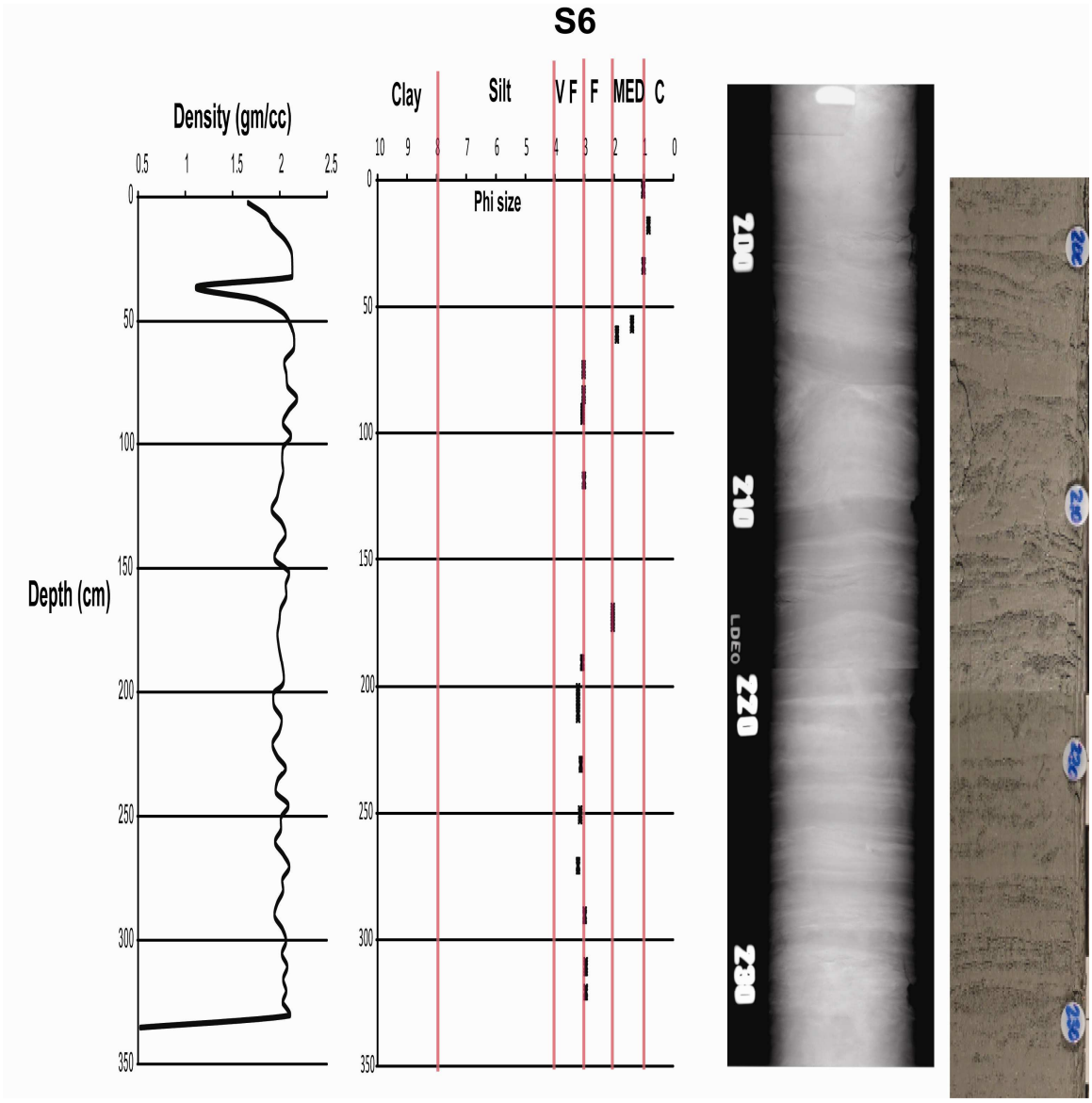

.

Figure 10: Graph (left) showing bulk density (gm/cc) versus depth (cm), alongside grain size (φ) versus depth (cm) for core S6 (see Figure 2b for location). Bulk density was acquired aboard the *R/V Knorr* as cores were brought onboard during the 2007 cruise. Black dots represent sampled intervals. VF= very fine, F = fine, MED = medium, C= coarse. Analog X-ray image (right) and photo of segment of core S6 provided by Lamont Doherty core facility. Analog X-rays showing mm to cm scale, alternating lamination of darker and lighter bands (~220-230cm) as well as other sedimentary structures with concave up and concave down geometries(~220-200cm).

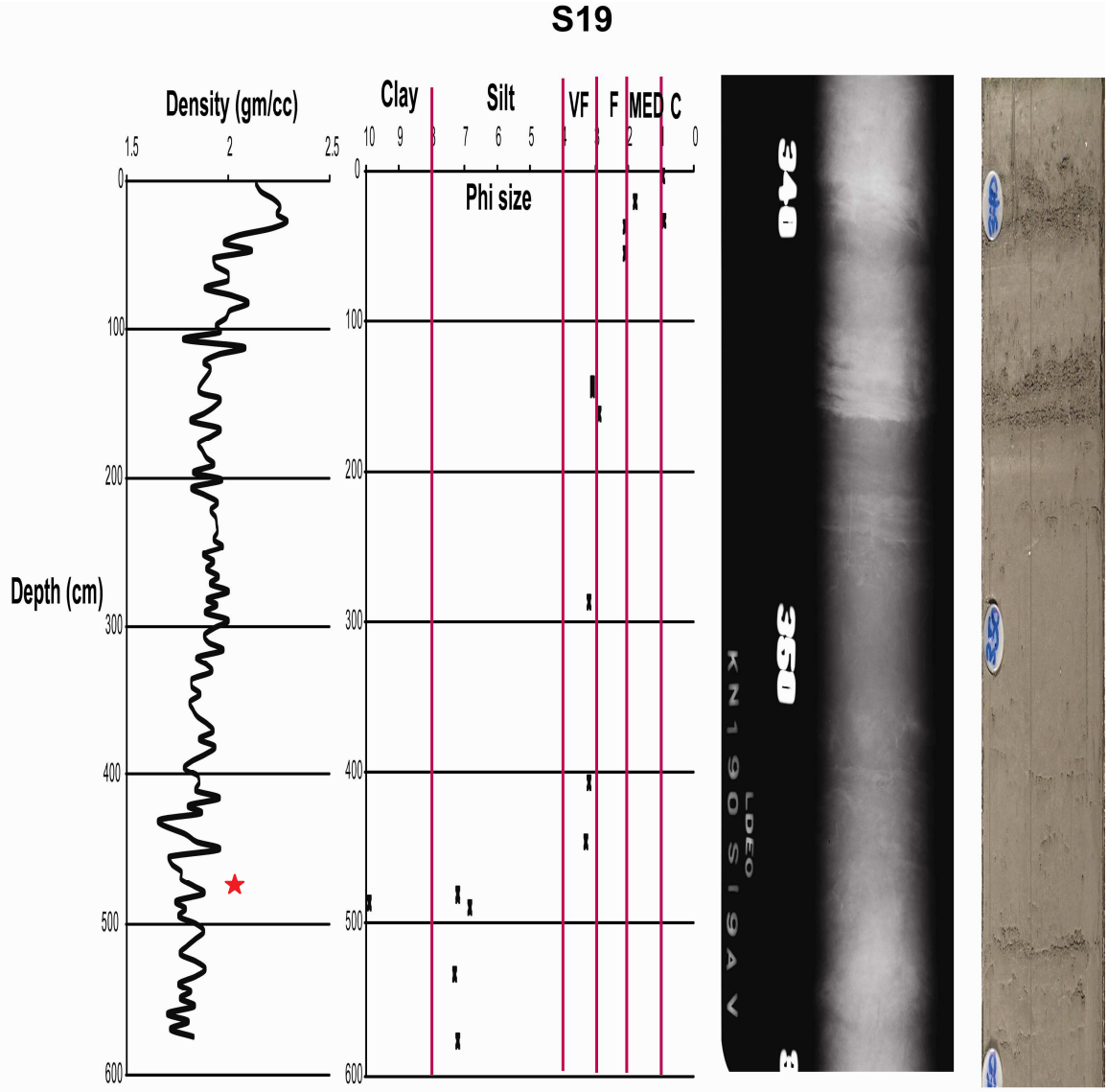

Figure 11: Graph (left) showing bulk density (gm/cc) versus depth (cm), alongside grain size (φ) versus depth (cm) for core S19 (see Figure 2b for location). Bulk density was acquired aboard the *R/V Knorr* as cores were brought onboard during the 2007 cruise. Black dots represent sampled intervals. VF= very fine, F = fine, MED = medium, C= coarse. Analog X-ray image (right) and photo of segment of core S19 provided by Lamont Doherty core facility. Analog X-rays showing mm scale lamination of darker and lighter strata atop a darker ~10cm darker strata near the base of the core. Red star denotes position of shell fragment aged at 10,247 +- 90 years BP.

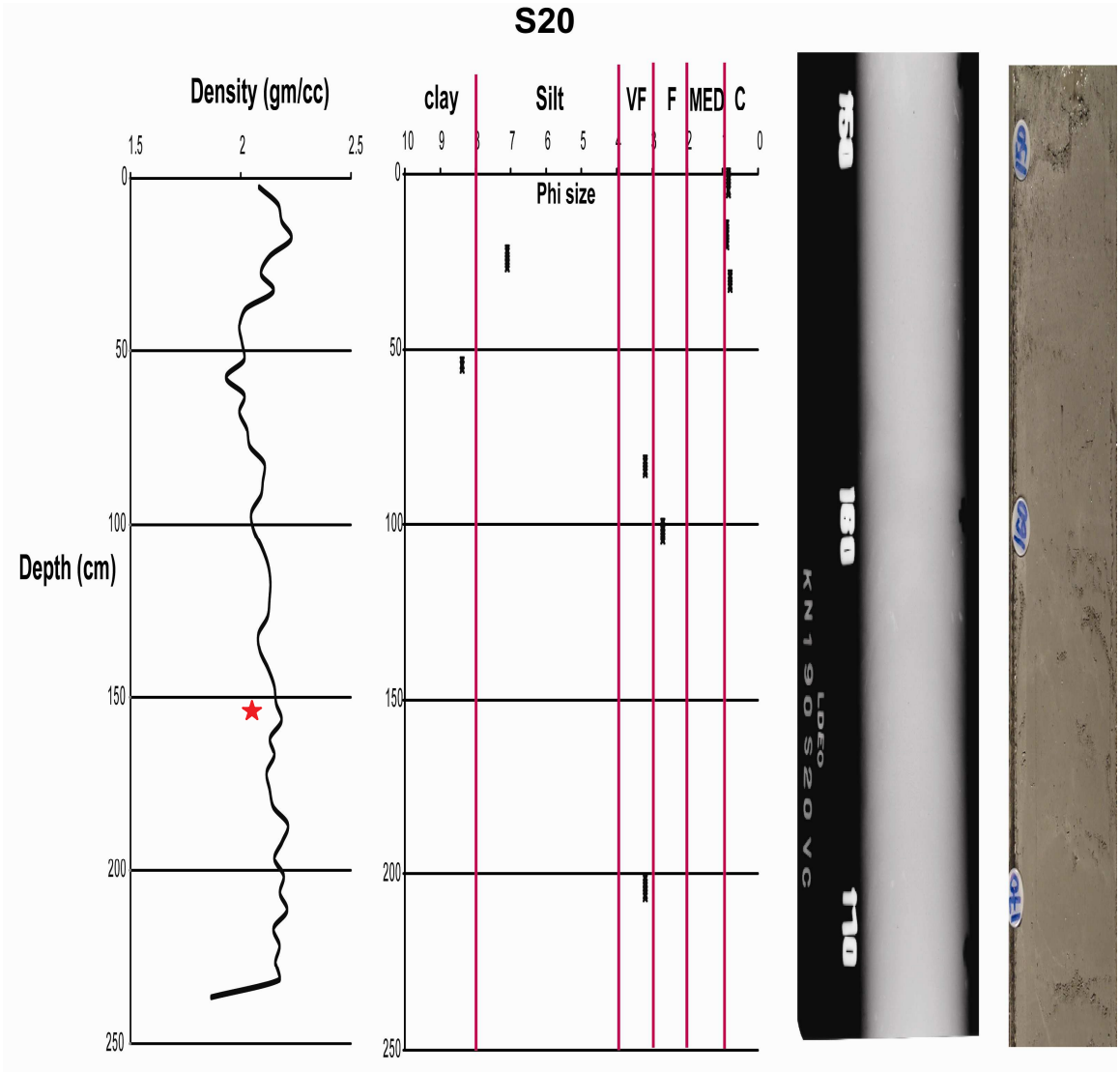

Figure 12: Graph (left) showing bulk density (gm/cc) versus depth (cm), alongside grain size (φ) versus depth (cm) for core S20 (see Figure 2b for location). Bulk density was acquired aboard the *R/V Knorr* as cores were brought onboard during the 2007 cruise. Black dots represent sampled intervals. VF= very fine, F = fine, MED = medium, C= coarse. Analog X-ray image (right) and photo of segment of core S20 provided by Lamont Doherty core facility. Analog X-rays does not display sedimentary structures, only massive, relatively homogeneous deposit. Red star denotes carbonate mud sampled aged at 40,734 +/- 686 years BP.

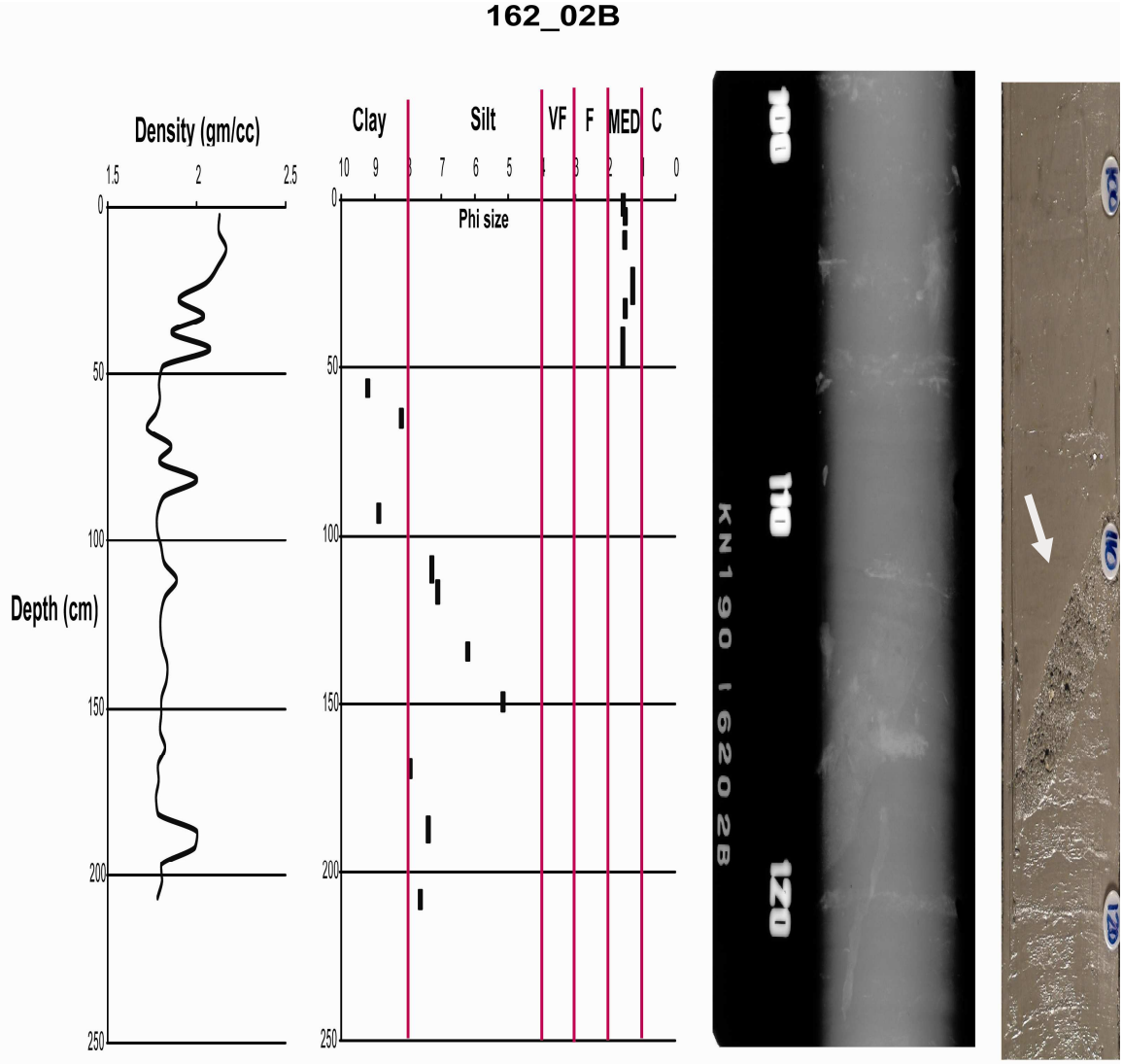

Figure: 13 Graph (left) showing bulk density (gm/cc) versus depth (cm), alongside grain size (φ) versus depth (cm) for core 162_02B (see Figure 2a for location). Bulk density was acquired aboard the *R/V Knorr* as cores were brought onboard during the 2007 cruise. Black dots represent sampled intervals. VF= very fine, F = fine, MED = medium, C= coarse. Analog X-ray image (right) and photo of segment of core 162_02B provided by Lamont Doherty core facility. Analog X-rays showing relatively structure-less deposit, white arrow pointing to a sand lense that is possibly a burrow.

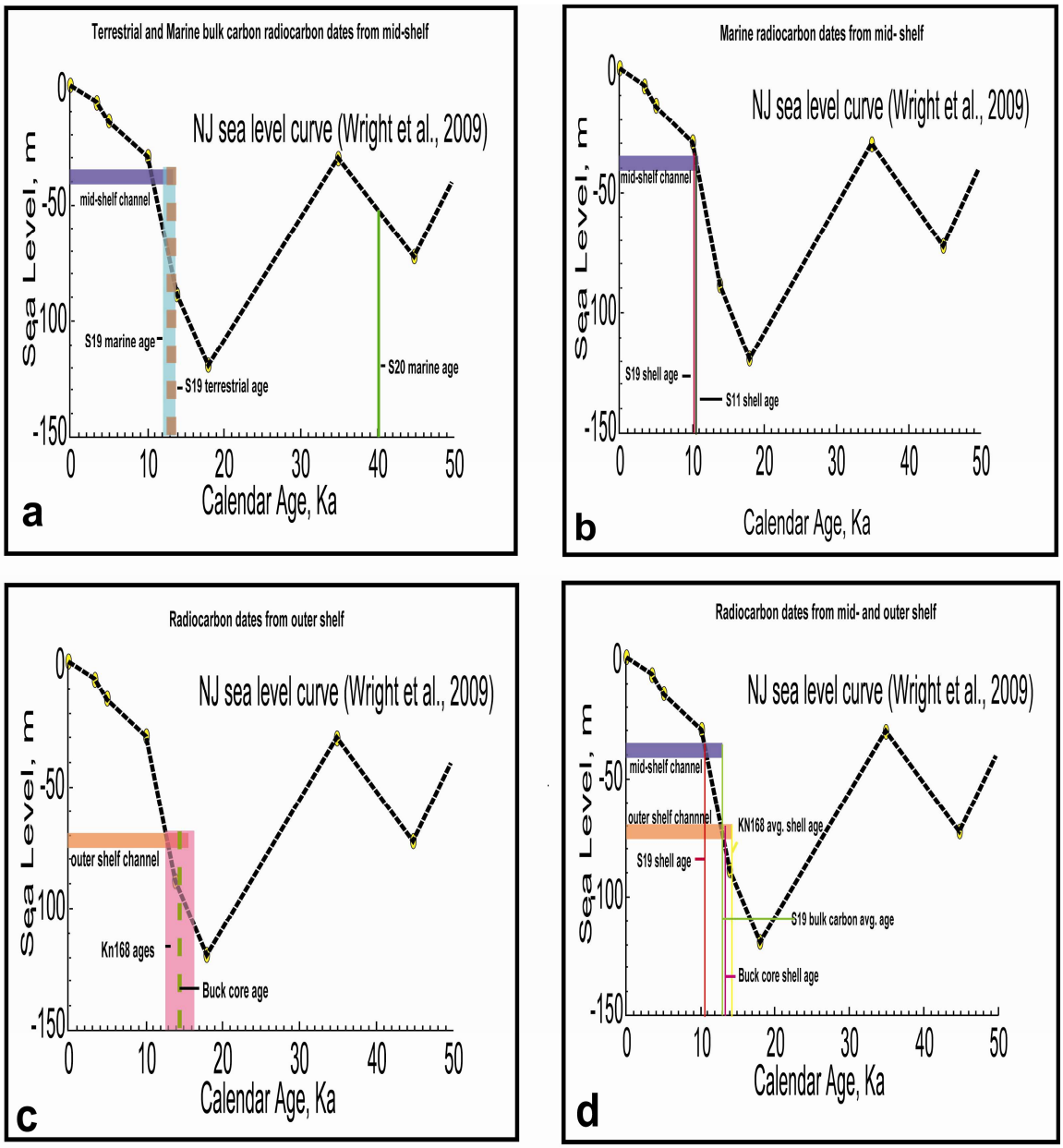

Figure 14: Diagrams showing radiocarbon dates for the mid- and outer shelf imposed on the New Jersey sea level curve from Wright et al., (2009). (a) Terrestrial and marine bulk carbon radiocarbon dates from the mid-shelf. (b) Marine radiocarbon dates from the mid-shelf. (c) Radiocarbon dates from previous studies on the outer shelf. Christensen et al., dates on wood and shell material are denote by research cruise name (KN168). (d) Radiocarbon dates from mid- and outer shelf. It is significant to note the difference between channel depths and age dates as signals for reworking of the sediment along the shelf. Mid- and outer shelf channel depth ranges obtained from seismic stratigraphy.

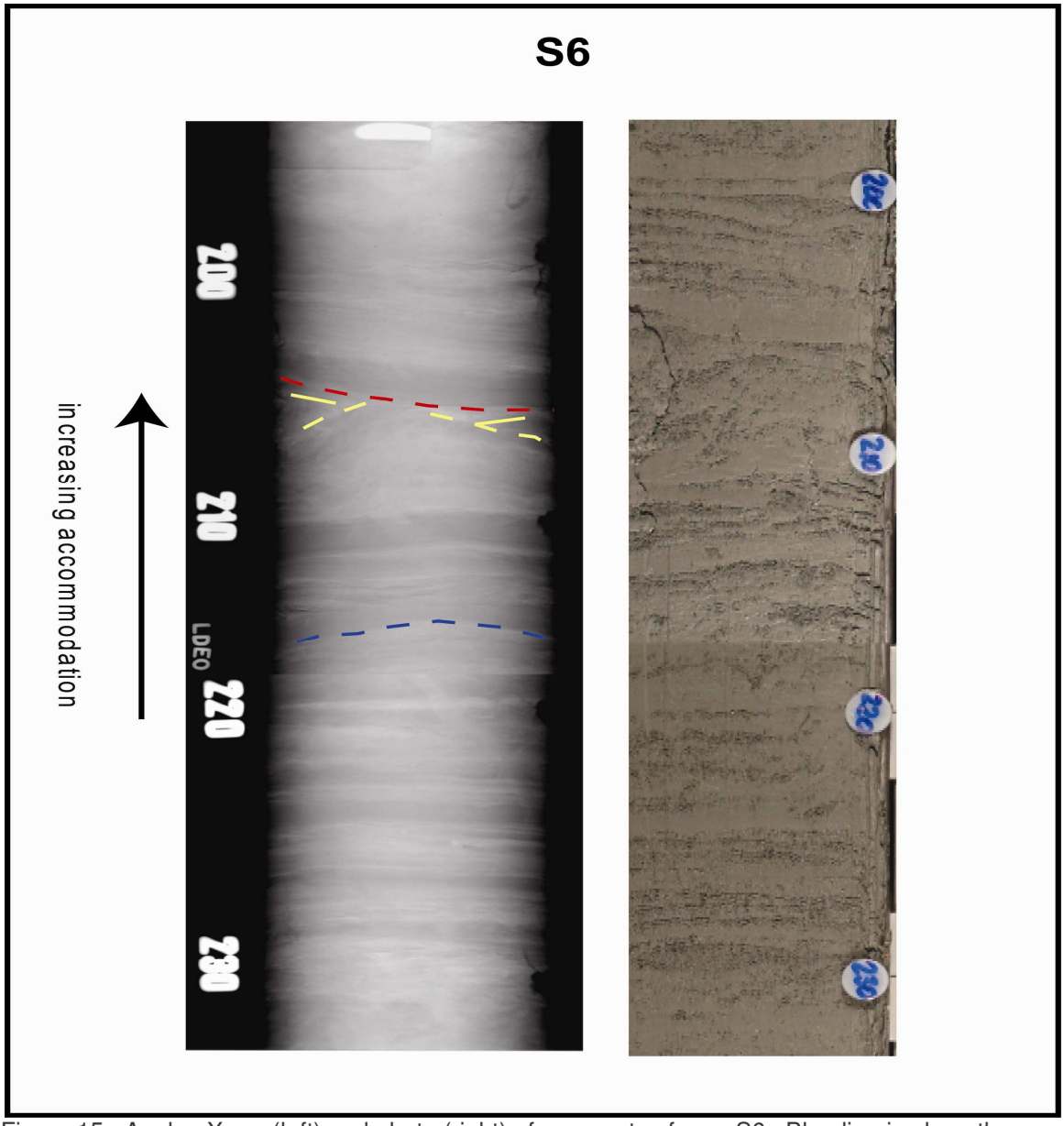

Figure 15: Analog X-ray (left) and photo (right) of segments of core S6. Blue line is along the surface of possible hummocky structure, suggesting that deposition within the channel was proximal to the shoreline and was under wave and tidal influenced conditions. Yellow lines are atop the area of apparent deformation, suggesting that there was a rapid influx of a large amount of sediment into the system. Red line shows base of truncating strata, suggesting that the large influx of sediment was rapid and dense enough to erode the underlying sediment as it enter the channel. Throughout the core, there is an overall increase in accommodation suggesting that sea level was rising steadily. Photos and X-rays provided by Lamont Doherty core facility.

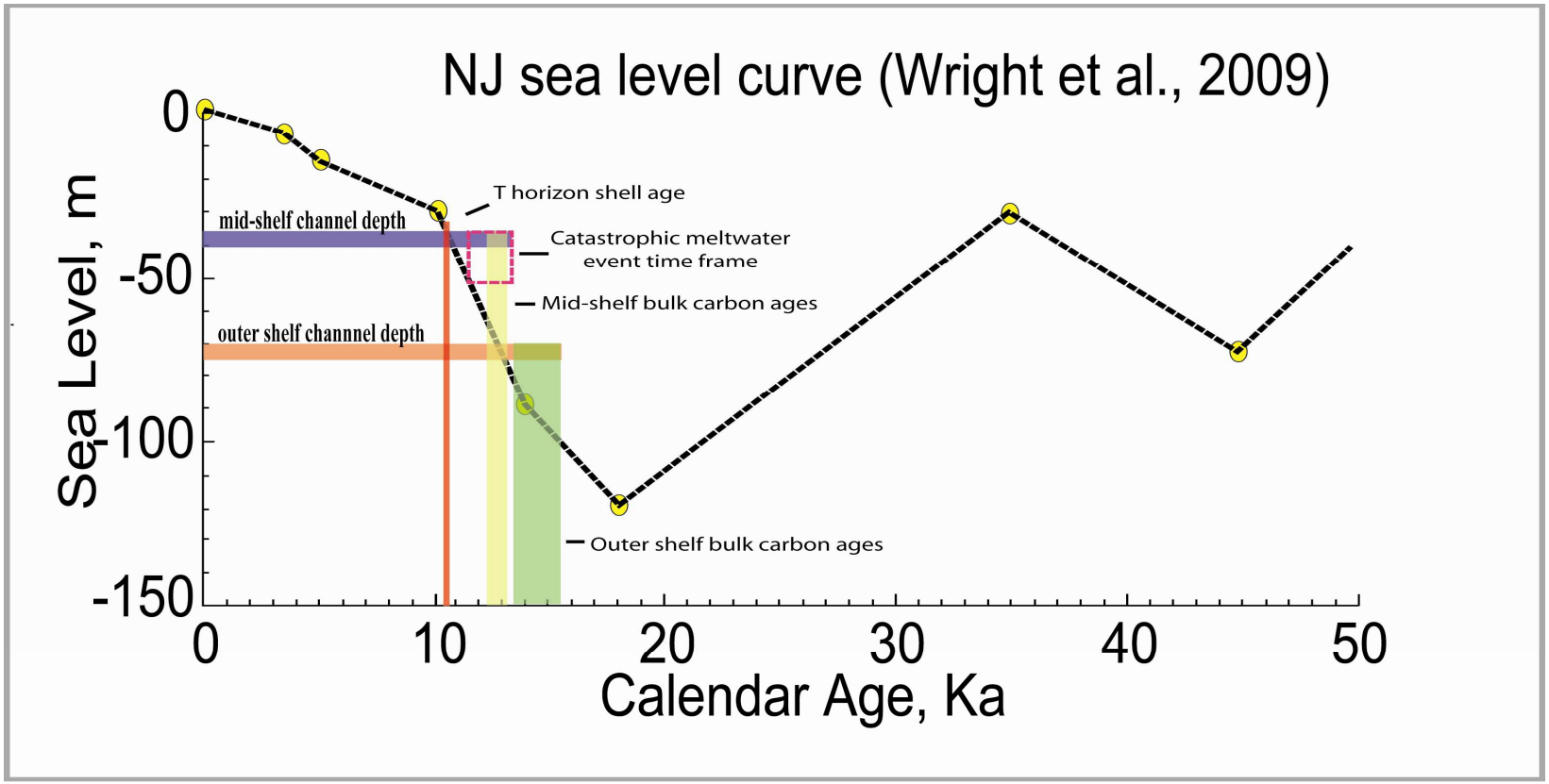

Figure 16: Diagram showing radiocarbon dates from mid- and outer shelf, imposed on the New Jersey sea level curve from Wright et al., (2009). Mid-shelf and outer shelf channel depth ranges obtained from seismic stratigraphy. Sea level depth in meters. Dashed box shows constraint of time of catastrophic meltwater flood event (Theiler et al., (2007).

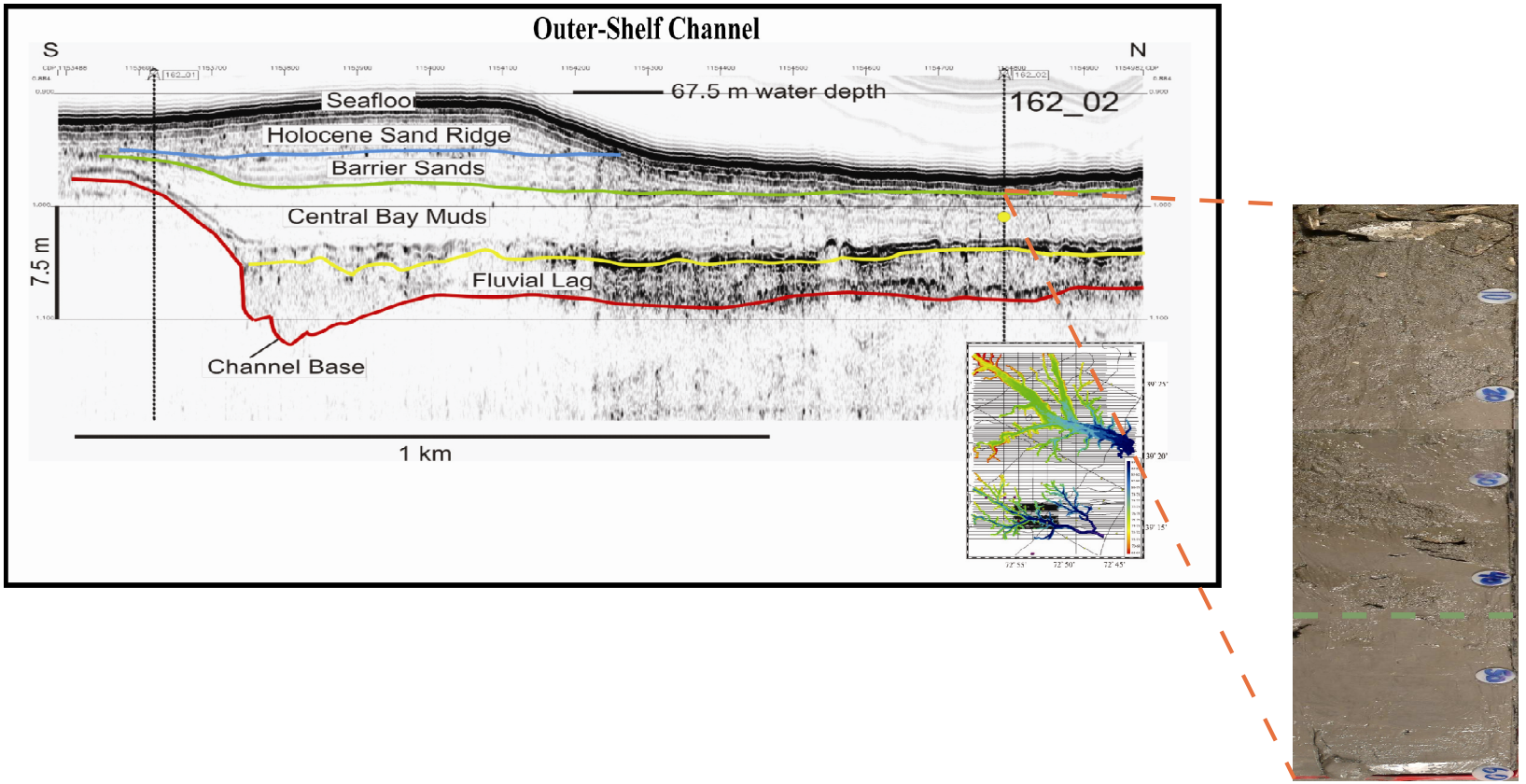

Figure 17: Stratigraphy of the outer-shelf channel that is positioned in ~70-80 meters water depth. Flat lying reflectors have been interpreted by Nordfjord et al., (2006) as a well ordered sequence with identifiable reflectors. Also includes map of outer-shelf channel system interpreted by Nordfjord et al., (2006), see also Figure 3. Photo (right) of 0-40 cm interval of core 162_02B by Lamont Doherty Earth Observatory showing possible transition from barrier sands (above) to central basin muds (below). VE = ~25

Bibliography

Allen, G.P., and Posamentier, H.W., 1993, Sequence stratigraphy and facies model of an incised valley fill: the Gironde Estuary, France: Journal of Sedimentary Petrology, v. 63, p. 378–391.

Amorosi, A., Colalongo, M. L., Dinelli, E., Lucchini, F., Vaiani, S.C., 2007, Cycle variation in sediment provenance from late Pleistocene deposits of eastern Po Plain, Italy. In Arribas, J., Critelli, S., and Johnsson, M.J., eds., Sedimentary Provenance and Petrogenesis: Perspectives from Petrography and Geochemistry: Geological Society of America Special Paper 420. p. 13-24

Austin, J.A., C.S. Fulthorpe, G.S. Mountain, D.L. Orange and M.E. Field, 1996: Continental-margin seismic stratigraphy: assessing the preservation potential of heterogeneous geologic processes operating on continental shelves and slopes. *Oceanography, 9,* p. 173-177.

Blum, M.D. and T.E. Tornqvist, 2000, Fluvial responses to climate and sea-level change; a review and look forward: Sedimentology, v. 47, supplement 1, p. 2-48.

Boyd, R., Dalrymple, R.W., and Zaitlin, B.A., 1992, Classification of coastal sedimentary environments: Sedimentary Geology, v. 8-0, p. 139-150.

Buck, K.F., Olson, H.C., and Austin, J.A., JR., 1999, Paleoenvironmental evidence for latest Pleistocene sea level fluctuations on the New Jersey outer continental shelf: combining high-resolution sequence stratigraphy and foraminiferal analysis: Marine Geology, v. 154, p. 287–304.

Christensen, B.A., Alexander, C., Stackhouse. S.B., Turner, J., Nordfjord, S., Austin, J.A., JR., Goff, J.A., Gulick, S., Fulthorpe, C., Late Pleistocene deposition and erosion on the New Jersey shelf, 2007, AGU abstract

Curray, J.R., 1964, Transgression and regression, *in* Miller, R.L., ed., Papers in Marine Geology, Shepard Commemorative Volume: New York, Macmillan, p. 175-203

Davies, T.A., Austin, J.A., JR., Lagoe, M.B., and Milliman, J.D., 1992, Late Quaternary sedimentation off New Jersey: New results using 3-D seismic profiles and cores: Marine Geology, v. 108, p. 323–343.

Dalrymple, R.W., Boyd, R., and Zaitlin, B.A, 1994, Incised valleys: origin and sedimentary sequences, Society for Sedimentary Geology Special Publication No. 85, 348 p.

Dalrymple, R.W., Boyd, R., and Zaitlin, B.A, 2006, Incised valleys in time and space, Society for Sedimentary Geology Special Publication No. 85, 348 p.

Dalrymple, R.W., Boyd, R., and Zaitlin, B.A., 1992, Estuarine facies model: conceptual basis and stratigraphic implications, Journal of Sedimentary Petrology, v. 62, no. 6, p. 1130-1146.

Dalrymple, R.W., Boyd, R., and Zaitlin, B.A., 1994, History of research, valley types and internal organization to the volume, *in* Dalrymple, R.W., Boyd, R., Zaitlin, B.A., eds., Incised-Valley Systems: Origin and Sedimentary Sequences: SEPM Special Publication 51, p. 3-10

Donnelly, J.P., Driscoll, N.W., Uchupi, E., Keigwin, L.D., Schwab, W.C., Thieler, E.R., Swift, S.A., 2005, Catastrophic meltwater discharge down the Hudson Valley: A potential trigger for the Intra Allerod cold period, Geology, v. 33, p. 89-92

Duncan, C. S., J. A. Goff, J. A. Austin, and C. S. Fulthorpe, 2000,Tracking the last sea level cycle: Seafloor morphology and shallow stratigraphy of the latest Quaternary New Jersey middle continental shelf, *Mar. Geol.*, *170*, p.395-421

Duncan, C. S., 2001. Late Quaternary Stratigraphy and Seafloor Morphology of the New Jersey Continental Shelf. PhD. Thesis, University of Texas, 222 pp.

Ewing, J., X.l. Pichon, and M. Ewing, 1963, Upper stratification of Hudson apron region: Journal of Geophysical Research, v. 68, p. 6303-6316.

Fairbanks, R.G., R.A. Mortlock, T.-C. Chiu, L. Cao, A. Kaplan, T.P. Guilderson, T.W. Fairbanks and A.L. Bloom, 2005. Marine Radiocarbon Calibration Curve Spanning 10,000 to 50,000 Years B.P. Based on Paired $^{230}Th/^{234}U/^{238}U$ and ^{14}C Dates on Pristine Corals. *Quaternary Science Reviews*, 24, p.1781-1796.

Folk, R. L., 1974, Petrology of Sedimentary Rocks: Austin, Texas, Hemphill Publishing Company, 182 p.

Fry, B., and E. Sherr. 1984. d13C measurements as indicators of carbon flow in marine and freshwater ecosystems. Contrib. Mar. Sci. 27, p. 15-47.

Fulthorpe, C.S., Austin, J.A, 2004, Shallowly buried, enigmatic seismic stratigraphy on the New Jersey outer shelf: Evidence for latest Pleistocene catastrophic erosion, Geology., v. 32. No. 12, p. 1013-1016

Galloway, W. E., and Hobday, D. K., 1996, Terrigenous clastic depositional systems: Heidelberg, Springer-Verlag, 489 p.

Goff, J.A., Swift, D.J.P., Duncan, C.S., Mayer, L.A., and Hughes-Clarke, J., 1999, High-resolution swath sonar investigation of sand ridge, dune and ribbon morphology in the offshore environment of the New Jersey margin: Marine Geology, v. 161, p. 307–337.

Gulick, S.P.S., Goff, J.A., Austin, J.A., JR., Alexander, C.R., Nordfjord, S., and Fulthorpe, C.S., 2005, Basal inflection-controlled shelf-edge wedges off New Jersey track sea-level fall: Geology, v. 33, p. 429–432.

Harris, J.D., 1983. Pleistocene events from the shallow structure of the middle and outer continental shelf of New Jersey. Masters Thesis, University of Rhode Island, Providence, RI, p. 1-112.

Hathaway, J.C., C.W. Poag, P.C. Valentine, R.E. Miller, D.M. Schultz, F.T. Manheim, F.A. Kohout, M.H. Bothner, and D.A. Sangrey,1979, The U.S. Geological Survey core drilling on the U.S. Atlantic Shelf. *Science* 206, no. 4418, p. 515–527.

Knebel, H.J., 1977 E. Spiker, 1977, Thickness and age of surficial sand sheet, Baltimore Canyon trough area: American Association of Petroleum Geologist Bulletin, v. 61, p. 861-871

Knott, S.T., and H. Hoskins, 1968, evidence of Pleistocene events in the structure of the continental shelf off north eastern United States: Marine Geology, v. 6, p. 5-43.

Lagoe, M.B., Davies, T.A., Austin Jr., J.A., Olson, H.C., 1997. Foraminiferal constraints on very high-resolution seismic stratigraphy and Late Quaternary history, New Jersey continental shelf. Palaios 12, p. 249–266.

Masselink, G., and Hughes, M.G., 2003, Introduction to Coastal Processes and Geomorphology: New York, Oxford University Press, 354 p.
Milliman, J.D., Jiezao, Z., Anchun, L., and Ewing, J.I., 1990, Late Quaternary sedimentation on the outer and middle New Jersey continental shelf: Results of local deglaciation: Journal of Geology, v. 98, p. 966–976.
Muller, E.H., Prest, V.K., 1985. Glacial Lakes in the Ontario basin. In: Karrow, P.F., Calkin, P.E. (Eds.), Quaternary Evolution of the Great Lakes. Geological Association of Canada Special Paper, vol. 30, p. 213–229.
Nordfjord, S., Goff, J.A., Austin, J.A., JR., Sommerfield, C.K., 2005, Seismic geomorphology of buried channel systems on the New Jersey outer shelf: Assessing past environmental conditions: Marine Geology, v. 214, p. 339–364.
Nordfjord, S., Goff, J. A., Austin, J. A., Jr., Gulick, S. P. S. 2006, Seismic Facies of Incised-Valley Fill, New Jersey Continental Shelf: Implications of Erosion and Preservation Processes Acting During Latest Pleistoncene-Holocence Transgression: Journal of Sedimentary Research, v. 76, p. 1284-1303.
Pair, D.L., Rodrigues, C.G., 1993. Late Quaternary deglaciation of the southwestern St. Lawrence Lowland, New York and Ontario. Geological Society of America Bulletin 105, p. 1151–1164.
Poag, C. W., 1981, Ecologic atlas of benthic foraminifera of the Gulf of Mexico Mar. Sci. Int., Woods Hole, MA, United States 174 *pp.*
Pritchard, D.W., 1967, What is an estuary? Physical viewpoint, in Lauff, G.H., ed., Estuaries: American Association for the Advancement of Science, Publication 83, p. 3-5.
Ridge, J.C., 1997. Shed Brook Discontinuity and Little Falls Gravel: evidence for the Erie interstade in central New York. Geological Society of America Bulletin 109, p. 652–665.
Schlee, J., and R.M. Pratt, 1970, Atlantic continental shelf and slope of the United States- gravels of the northeastern part: Geological Survey Profession Paper, v. 529-H, p. 1-29.
Schumm, S.A., 1977, the Fluvial System: New York, John Wiley, p. 338
Schumm, S.A., and Ethridge, F.G., 1994, Origin, Evolution and Morphology of Fluvial Valleys, in Dalrymple, R.W., Boyd, R., Zaitlin, B.A., eds., Incised-Valley Systems: Origin and Sedimentary Sequences: SEPM Special Publication 51, p. 11-27
Sheridan, R.E., Ashely, G.M., Miller, K.G., Waldner, J.S., Hall, D.W., and Uptegrove, J., 2000, Offshore–onshore correlation of upper Pleistocene strata, New Jersey Coastal Plain to continental shelf and slope: Sedimentary Geology, v. 134, p.197–207.
Stanford, S.D., Harper, D.P., 1991. Glacial lakes of the lower Passaic, Hackensack, and lower Hudson valleys, New Jersey and New York. Northeastern Geology 13, p. 271–286.
Stone, B.D., and H.W. Borns, V.Sibrava, D.Q. Bowen, and G.M. Richmond, eds., 1986, Pleistocene glacial and interglacial stratigraphy of New England, Long Island and adjacent Georges Bank and Gulf of Maine, in Quaternary Glaciations of the Northern Hemisphere: Quaternary Science Review, p. 39-52.

Stuiver, M. and P.J. Reimer 1993 Extended 14C data base and revised CALIB 3.0 14C Age calibration program *Radiocarbon* **35**(1), p. 215-230

Swift, D.J.P., Moir, R., and Freeland, G.L., 1980, Quaternary Rivers on the New Jersey shelf: relation of seafloor to buried valleys: Geology, v. 8, p. 276–280.

Thieler, R.A., Butman, B., Schwab, W.C., Allison, M.A., Driscoll, N.W., Donnelly, J.P., Uchupi, E., 2007, A catastrophic meltwater flood event and the formation of the Hudson Shelf Valley: Paleography, vol. 246, no. 1, p. 120-136

Wood, J.M., Hopkins, J.C. 1989, Reservoir sandstone bodies in estuarine valley fill: lower Cretaceous Glauconitic member, Little Bow Field, Alberta, Canada: American Association of Petroleum Geologists Bulletin, v. 37, p. 1361-1382

Wright, J.D., Sheridan, R.E, Miller, K.G., Uptegrove, J., Cramer, B.S., and Browning, J.V., 2009, Late Pleistocene sea level on the New Jersey Margin: Implications to eustasy and deep-sea temperature: Global and Planetary Change, v. 66, p. 93

Zaitlin, B.A., Boyd, R., and Dalrymple, R.W., 1994, The stratigraphic organization of incised-valley systems associated with relative sea-level change, *in* Dalrymple, R.W., Boyd, R., Zaitlin, B.A., eds., Incised-Valley Systems: Origin and Sedimentary Sequences: SEPM Special Publication 51, p. 3-10

VITA

Stanley Bernard Stackhouse was born in Thomaston, Georgia on June 5, 1984, the son of Shirley Denise Stackhouse and Stanley Stackhouse. After completing his work at Upson-Lee High School, Thomaston, Georgia, 2002, he entered Fort Valley State University in Fort Valley, Georgia as a chemistry major. In the Fall of 2005, he transferred to the University of Texas at Austin in Austin, Texas and enrolled as a general geology major. He received a Bachelor of Science in General Geology from UT Austin in August of 2007 and a Bachelors of Science in Chemistry from Fort Valley State University in May of 2008. He entered graduate school at UT Austin in the August of 2009.

Permanent Address: 1263 Spring Street
Thomaston, GA 20386

This thesis was typed by Stanley B. Stackhouse.